



1 **ARIOS: An acidification ocean database for the Iberian Upwelling Ecosystem**  
2 **(1976 - 2018)**

3  
4 **Xosé Antonio Padin\*<sup>1</sup>, Antón Velo<sup>1</sup> and Fiz F. Pérez<sup>1</sup>**

5 <sup>1</sup> Instituto de Investigaciones Marinas, IIM-CSIC, 36208 Vigo, Spain.

6 [padin@iim.csic.es](mailto:padin@iim.csic.es), [avelo@iim.csic.es](mailto:avelo@iim.csic.es), [fiz.perez@iim.csic.es](mailto:fiz.perez@iim.csic.es)

7

8 **1. Abstract**

9 A data product of 17,653 discrete samples from 3,343 oceanographic stations  
10 combining measurements of pH, alkalinity and other biogeochemical parameters off the  
11 North-western Iberian Peninsula from June 1976 to September 2018 is presented in this  
12 study. The oceanography cruises funded by 24 projects were primarily carried out in the  
13 *Ría de Vigo* coastal inlet, but also in an area ranging from the Bay of Biscay to the  
14 Portuguese coast. The robust seasonal cycles and long-term trends were only calculated  
15 along a longitudinal section, gathering data from the coastal and oceanic zone of the  
16 Iberian Upwelling System. The pH in the surface waters of these separated regions,  
17 which were highly variable due to intense photosynthesis and the remineralization of  
18 organic matter, showed an interannual acidification ranging from  $-0.0016 \text{ yr}^{-1}$  to  $-0.0032$   
19  $\text{yr}^{-1}$  that grew towards the coastline. This result is obtained despite the buffering  
20 capacity increasing in the coastal waters further inland as shown by the increase in  
21 alkalinity by  $1.1 \pm 0.7 \mu\text{mol kg}^{-1} \text{ yr}^{-1}$  and  $2.6 \pm 1.0 \mu\text{mol kg}^{-1} \text{ yr}^{-1}$  in the inner and outer *Ría*  
22 *de Vigo* respectively, driven by interannual changes in the surface salinity of  
23  $0.0193 \pm 0.0056 \text{ psu yr}^{-1}$  and  $0.0426 \pm 0.016 \text{ psu yr}^{-1}$  respectively. The loss of the vertical  
24 salinity gradient in the long-term trend in the inner ria was consistent with other  
25 significant biogeochemical changes such as a lower oxygen concentration and  
26 fertilization of the surface waters. These findings seem to be related to a growing  
27 footprint of sediment remineralization of organic matter in the surface layer of a more  
28 homogeneous water column.

29 Data are available at: <http://dx.doi.org/10.20350/digitalCSIC/12498> (Pérez et al., 2020).

30

31 **2. Introduction**

32 CO<sub>2</sub> emissions of anthropogenic origin (fossil fuels, land use and cement  
33 manufacturing) into the atmosphere are the main cause behind the warming of the Earth  
34 due to the greenhouse effect (IPCC, 2013). Given the constant exchange of gases



35 through the air-sea interface, the oceanic reservoir plays a key role as a sink for about  
36 31% of anthropogenic CO<sub>2</sub> emissions (Sabine et al., 2004), controlling the partial  
37 pressure of carbon dioxide in the atmosphere and regulating global temperatures.

38

39 The CO<sub>2</sub> uptake by the oceans produces changes in the inorganic carbon system in spite  
40 of being partially dampened by the seawater buffering capacity. This ability of seawater  
41 to fix anthropogenic CO<sub>2</sub> becomes more limited as more CO<sub>2</sub> is absorbed, which will  
42 make it difficult to stabilize atmospheric CO<sub>2</sub> in the future (Orr et al., 2009). In any  
43 case, the rapid increase of CO<sub>2</sub> in the atmosphere decreases the ocean's pH (Caldeira  
44 and Wickett, 2003; Raven et al., 2005). This effect of CO<sub>2</sub> absorption, which is known  
45 as ocean acidification, conditions the buffering capacity of seawater and to some extent  
46 the exchange of CO<sub>2</sub> between the ocean and the atmosphere. The Intergovernmental  
47 Oceanographic Commission of the United Nations identified the chemical change in  
48 seawater brought about by ocean acidification as an indicator of a stressor on marine  
49 ecosystems with a negative impact on socio-economic activities such as fishing and  
50 shellfish farming. Hence, it was necessary for the oceanography community to observe  
51 and gather data about pH and other parameters of the marine carbon system to produce  
52 global and regional data products in order to help sustainably manage the ocean's  
53 resources.

54

55 The threat of oceanic acidification of marine ecosystems is especially significant in  
56 regions like coastal upwelling areas, which are more sensitive and appear to respond  
57 faster to anthropogenic perturbations (Feely et al., 2008; Gruber et al., 2012; Lachkar,  
58 2014; Hauri et al., 2013). These ecosystems are characteristic for their complex physical  
59 and biogeochemical interactions and for sustaining enormous biological productivity  
60 and productive fisheries (Pauly and Christensen, 1995; Haury et al., 2009). The  
61 photosynthetic activity in these regions is also an important mechanism for the seawater  
62 CO<sub>2</sub> uptake, converting most of these areas into atmospheric CO<sub>2</sub> sinks (Pérez et al.,  
63 1999; Cobo-Viveros et al., 2013). However, the great spatial and temporal variability  
64 has been widely spaced and intermittent over time, preventing a complete view from  
65 being obtained of ocean acidification in the upwelling system.

66

67 The effects of ocean acidification on marine ecosystems has awoken the interest of the  
68 international community and has stimulated global impetus for gathering high quality



69 time-series measurements of the marine inorganic carbon system (Hofmann et al., 2011;  
70 Andersson and MacKenzie, 2012; McElhany and Busch, 2013; Takeshita et al., 2015;  
71 Wahl et al., 2016) and for predicting the future evolution of the pH caused by climate  
72 change. Researchers at the *Instituto de Investigaciones Mariñas* (IIM-CSIC) in Vigo  
73 (Spain) have already started this task, measuring the marine inorganic carbon system  
74 and associated parameters on the Galicia coast in the northwest of the Iberian Peninsula,  
75 since 1976. These biogeochemical changes, including the pH variation, have been  
76 gathered via different projects with particular objectives between 40°N and 45°N, 11°W  
77 and the Galician coast over the past 40 years. The current database, hereinafter called  
78 ARIOS (Acidification in the rias and the Iberian continental shelf) database, holds  
79 biogeochemical information from 3,357 oceanographic stations, giving 17,653 discrete  
80 samples. This unique collection is a starting point for evaluating the ocean acidification  
81 in the Iberian Upwelling System characterized by intense biogeochemical interactions  
82 as an observation-based analysis, or for use as inputs in a coupled physical-  
83 biogeochemical model to disentangle these interactions at the ecosystem level.

84

### 85 **3. Data provenance**

#### 86 **3.1. Region**

87 The main characteristic of the Galician coastline, located in the north-west of the  
88 Iberian Peninsula, is the *Rías Baixas*, four long coastal estuaries or rias ( $>2.5 \text{ km}^3$ )  
89 between 42°N and 43°N (Fig. 1). The water exchange between the *Rías Baixas* and open  
90 waters is drastically affected by the coastal wind pattern as part of the Canary Current  
91 Upwelling System (Wooster et al., 1976; Fraga 1981; Aristegui et al., 2004). Under the  
92 predominance of northeasterly winds (Blanton et al., 1984) during spring-summer, the  
93 surface offshore transport of surface waters leads to a rising cold, nutrient-rich, deep  
94 water mass called the Eastern North Atlantic Central Water (ENACW) (Ríos et al.,  
95 1992). Under these conditions, the *Rías Baixas* act as an extension of the continental  
96 shelf (Rosón et al., 1995; Souto et al., 2003; Gilcoto et al., 2017), where upwelling  
97 filaments extending westward export primary production from the coast into the ocean  
98 (Álvarez-Salgado et al., 2001). In the opposite direction, the prevalence of northward  
99 winds (Blanton et al., 1984) moves the surface waters towards the coast, where they  
100 accumulate, sink and thus isolate the coast. This process, known as downwelling, is  
101 typical during the autumn-winter along with other characteristics such as the warm,  
102 salty waters from the Iberian Poleward Current (IPC) of subtropical origin (Fraga et al.,



103 1982; Alvarez-Salgado et al., 2006) that flows constrained to the Iberian shelf break  
104 (Frouin et al., 1990). The run-off from local rivers also contributes to the presence of  
105 river plumes over the shelf (Otero et al., 2008). These hydrodynamic conditions, the  
106 meteorological forcings and the alternation of periods of upwelling and downwelling  
107 (Àlvarez, 1999; Gago et al., 2003c; Cobo-Viveros et al., 2013) stimulate the  
108 development of intense primary production and high rates of recycling and downward  
109 carbon export (Alonso-Pérez and Castro, 2014). The result of this biogeochemical  
110 variability in terms of air-sea CO<sub>2</sub> exchange is that the surface waters act as a net CO<sub>2</sub>  
111 sink that is especially intense and variable over the shelf compared to offshore or in the  
112 inner *Rías Baixas* (Padin et al., 2010).

113

114 In addition to the short-term and seasonal variability, significant changes in the long-  
115 term scale have been reported in this region. In addition to changes such as the  
116 weakening and shortening of the upwelling events (Lemos and Sansó, 2006; Pérez et  
117 al., 2010; Alvarez-Salgado et al., 2009), warming (González-Pola et al., 2005; Pérez et  
118 al., 2010) and changes in the composition of phytoplankton (Bode et al., 2009; Pérez et  
119 al., 2010), the acidification in the surrounding waters of the Galician coast has also been  
120 observed at a rate of -0.0164 pH units per decade in the first 700 metres (Ríos et al.,  
121 2001; Castro et al. 2009).

122

### 123 **3.2. Data sources**

124 The ARIOS database is a compilation of biogeochemical properties with discrete  
125 measurements of temperature, salinity, oxygen, nutrients, alkalinity, pH and chlorophyll  
126 that were sampled in waters off the northwest of the Iberian Peninsula from 1976 to  
127 2018 and measured by IIM-CSIC (Table 1). This data collection is part of the research  
128 by 24 projects and oceanographic cruises conducted in response to different aims. The  
129 different sampling strategies built up an irregular biogeochemical database whose  
130 particular frequency and spatial coverage is shown in Figure 2.

131

132 The contribution to the ARIOS database from the oceanographic cruises and projects  
133 over the different decades is described below.

134

#### 135 **Cruises in the 70s and 80s:**



136 The first three cruises were carried out over three periods (1976, 1981-1983 and 1983-  
137 1984), sampling the *Ría de Vigo*. These cruises were designed to provide environmental  
138 information (upwelling events, estuarine circulation, continental inputs, etc.) for  
139 research into the biology of some fish species. They measured identical parameters in  
140 the Vigo estuary but at different stations and frequency.

141

142 In the summer of 1984, the *Galicia VIII* cruise studied the summer upwelling events  
143 occurring on the contact front between the two ENACW water masses off Cape  
144 Finisterre from short sections perpendicular to the Galician coast with 85 stations  
145 offshore and 35 stations over the shelf. This cruise marked a milestone in the  
146 oceanographic research of IIM-CSIC because it was the first time that the parameters of  
147 the carbon system were measured on-board in offshore waters. Moreover,  
148 measurements of a particular station on the shelf break with a bottom depth of 600  
149 metres were taken every two days for a month, including two-day continuous  
150 samplings.

151

152 Two years later, the *Ria de Vigo 1986* sampled along the main axis of the *Ria de Vigo*  
153 in 7 monthly repetitions during the first half of the year in which the primary production  
154 and the organic matter exchange between the estuary and the shelf was studied in  
155 relation to the hydrographic regime. Shortly afterwards, the same topic was also  
156 researched by the *Galicia IX* project in September and October 1986 from 145 stations,  
157 50 of which were coastal and 80 located in ocean waters (Prego et al., 1990).

158

159 The following year, the 1987 *Provigo* project (Nogueira et al., 1997) initiated a periodic  
160 study from a fixed site (42°14.5'N, 8°45.8'W) located in the main channel in the middle  
161 zone of the *Ría de Vigo*. This oceanographic station was selected as suitable for  
162 evaluating the main processes that occur in the inner ria associated with external forcing  
163 changes (Rios, 1992; Figueiras et al., 1994). Although the *Provigo* project finished in  
164 1996, the fixed station was repeatedly included in subsequent cruises, extending the  
165 time series at this location until today, when it is currently sampled every week by  
166 INTECMAR ([www.intecmar.gal](http://www.intecmar.gal)). An example of the subsequent sampling repetition of  
167 this station occurred the following year when one of the three stations in the Vigo  
168 estuary in the *Luna 1988* project (Fraga et al., 1992) took a sample every two weeks to



169 study the environmental control over the phytoplankton populations throughout an  
170 annual cycle (February 1988 - February 1989).

171

172 At the end of 80s, the carbon system monitoring by the IIM-CSIC was extended to the  
173 *Ría de Arousa* throughout 1989 (Álvarez-Salgado et al., 1993; Perez et al., 2000) in  
174 order to learn the effect of upwelling on the water circulation pattern, community  
175 production and the fluxes and net budgets of biogenic constituents in this ria with the  
176 highest mussel production in Europe. For 5 months, 11 stations' samples were repeated  
177 twice a week in the ria that is the most productive, housing intense cultivation of  
178 mussels on rafts (Blanton et al., 1984).

179

#### 180 **Cruises of the 90s:**

181 In the first half of this decade, studying the phytoplankton communities was the  
182 oceanographic cruises' most relevant aim, concentrating particularly on harmful algae  
183 blooms. The hydrodynamic and biogeochemical conditions controlling the growth,  
184 development and migration of the phytoplankton were analysed both in the interior of  
185 the estuary and on the continental shelf.

186

187 For five days in September, the 1990 *Ría de Vigo* cruise (Figueiras et al., 1994) sampled  
188 five stations distributed along the longitudinal axis of the ria and one at the northern  
189 mouth. The next year, the cruise Galicia XI was carried out in May, sampling at 39  
190 stations along eight transects perpendicular to the coastline; and Galicia XII (Alvarez-  
191 Salgado et al., 1998, 2002, 2003; Castro et al., 1994) in September, sampling at 37  
192 oceanic stations and 7 coastal stations.

193

194 The *Ría de Vigo* cruise in 1993-4 (Miguez et al., 2001), with four stations using 24  
195 repetitions with a CTD-SBE25, investigated the hydrodynamic and biogeochemical  
196 effect on the evolution of phytoplankton communities in the *Ría de Vigo*. Six samples  
197 were taken in approximately two weeks corresponding to two different periods  
198 (27 September to 8 October 1993, and 6 March to 24 March 1994).

199

200 *Ría de Vigo* 1994-95 (Alvarez et al., 1999; Doval et al., 1998, 1997a, 1997b) and *Ría de*  
201 *Vigo* 1997 (Gago et al., 2003a, b, c) were two cruises that took place in the second half  
202 of the decade. These campaigns' objective was no longer the ecology of the plankton,



203 but the factors behind the variation of the carbon pools during the upwelling and  
204 downwelling events along the central axis of the *Ría of Vigo*. During the 1997 cruises  
205 on board the *B/O Mytilus*, a systematic observation of the pCO<sub>2</sub> was carried out for the  
206 first time in Spanish coastal waters, using an autonomous continuous system with  
207 additional measurements of temperature, salinity and chlorophyll.

208

#### 209 **Cruises in the 2000s and recent years:**

210 After a period of poor sampling at the end of 90s, the first decade of the 21<sup>st</sup> century  
211 gave new impetus to biogeochemical monitoring of Galician waters. As shown below,  
212 several projects dealt with various objectives, focussing on particular issues in the  
213 dynamics of these waters:

214

215 The DYBAGA project (Galician Platform's Annual Dynamics and Biochemistry: short-  
216 scale variation) (Álvarez-Salgado et al., 2006; Castro et al., 2006; Nieto-Cid et al.,  
217 2004) analysed the phenomena of upwelling and downwelling in the Galician shelf  
218 opposite the *Ría de Vigo* weekly and their impact on the different biogeochemical and  
219 carbon system variables including organic dissolved matter. Three stations were  
220 sampled weekly from May 2001 to April 2002 between the shelf break (1,200 m deep)  
221 to the middle of the *Ría de Vigo* (45 m deep).

222

223 The REMODA (Reactivity of dissolved organic matter in a coastal upwelling system)  
224 (Álvarez-Salgado et al., 2005; Piedracoba et al., 2005; Nieto-Cid et al., 2006) project  
225 concentrated on learning the origin and destination of dissolved organic matter in the  
226 *Ría de Vigo* as well. Three stations along the main axis of the *Ría de Vigo*, including the  
227 fixed station as the central one, took samples with short (3-4 days) and seasonal time  
228 scales.

229

230 The FLUVBE project (Coupling of benthic and pelagic fluxes in the *Ría de Vigo*) added  
231 to knowledge about the productivity and the benthic fluxes of oxygen and inorganic  
232 nutrients in the *Ría de Vigo* from 16 oceanographic surveys with four stations between  
233 April 2004 and January 2005.

234



235 The ZOTRACOS project studied the biogeochemical and hydrodynamic  
236 characterization of the coastal transition zone in NW Spain during the downwelling  
237 period (Teira et al., 2009).

238

239 The CRIA (Circulation in a RIA) (Barton et al., 2019) project examined the layout of  
240 the two-layer circulation and propagation of upwelled and downwelled waters in order  
241 to estimate the flushing and vertical velocities in the *Ría de Vigo* in repeated  
242 hydrographic surveys between September 2006 and June 2007 (Barton et al., 2015,  
243 2016; Alonso-Perez and Castro, 2014; Alonso-Perez et al., 2010; Alonso-Perez et al.,  
244 2015).

245

246 The RAFTING project (Impact of mussel raft cultivation on the benthic-pelagic  
247 coupling in a Galician ria) (Frojan et al., 2018; Frojan et al., 2016; Froján et al., 2014)  
248 assessed for the first time how mussel cultivation influences the quality of particular  
249 organic carbon fluxes in the *Ría de Vigo*. Over the four seasons, two stations were  
250 visited every two to three days during each period, meaning 24 oceanographic cruises in  
251 2007 and 2008.

252

253 The CAIBEX (Continental shelf-ocean exchanges in the marine ecosystem of the  
254 Canary Islands-Iberian Peninsula) (Villacieros-Robineau et al., 2019) project compared  
255 the dynamics and biogeochemical activity between the coastal zone and the adjacent  
256 ocean in the study zone during the summer upwelling events. As part of the CAIBEX  
257 project, a mooring at the LOCO (Laboratory of Ocean and Coastal Observation)  
258 (Zuñiga et al., 2016, 2017) site located on the continental shelf was deployed and visited  
259 monthly for one year to monitor the vertical profiles of biogeochemical variables.

260

261 After these projects were completed in 2009, new measurements were not provided  
262 until 2018. The aim of the ARIOS project (Acidification in the rias and on the Iberian  
263 continental shelf) was to evaluate the impact of ocean acidification and learn about  
264 potential impacts on the mussels and their adaptation (Lassoued et al., 2019) to the new  
265 climate change.

266

267 **3.3. Methods**





268 To assess of the level of acidification in the ocean adjacent to the Galician coast,  
269 variables of the carbon system (pH and alkalinity), nutrient concentration, dissolved  
270 oxygen, chlorophyll-a, salinity and temperature were measured in each cruise. The  
271 variables measured in each oceanographic cruise gathered in the ARIOS dataset are  
272 shown in Table 1. The main changes in the material and methods throughout these years  
273 are detailed below.

274

#### 275 **T-S measurements**

276 Temperatures from 1976 to 1984 were measured using a Wallace and Tiernan  
277 bathythermograph. Reversing thermometers were used, attached to the water samplers  
278 between 1984 and 1990, correcting the temperature between the protected and  
279 unprotected thermometers according to Anderson (1974). During those years, the depth  
280 was calculated from the thermometric readings, rounding the result off to the nearest  
281 ten. After 1990, different models of CTD instruments often containing other sensors  
282 were used to obtain the thermohaline profile.

283

284 The first measurements of salinity were determined with a Plessey Environmental  
285 Systems 6230N inductive salinometer calibrated with normal IAPSO water and  
286 calculated from the equations given in the NIO and UNESCO International  
287 Oceanographic Tables (1981). After using this equipment, the salinity was determined  
288 with an AUTOSAL 8400A inductive salinometer calibrated with normal IAPSO water  
289 whose estimated analytical error was 0.003, using the equations given by UNESCO  
290 (1981) as well. CTDs began to be used in 1990 to create the vertical salinity profiles,  
291 calibrated using the salinity samples, whose possible deviations in the measurements  
292 were estimated from the discrete measurements from the AUTOSAL salinometer.

293

#### 294 **pH measurements**

295 The pH measurements were originally taken with a Metrohm E-510 pH meter with a  
296 glass electrode and a Ag/ClAg reference one calibrated with 7.413 NBS buffer. All pH  
297 values were converted to values at 15 °C using the temperature correction from the  
298 Buch and Nynas tables published by Barnes (1959). In 1984, the method was modified  
299 and the temperature normalization was carried out following Pérez and Fraga (1987b).  
300 Two years later, the measurement equipment was the Metrohm E-654 pH meter with an  
301 Orion 81-04 Ross combined glass electrode, with the pH converted to the SWS scale



302 using the hydrogen activity coefficient given by Mehrbach et al. (1973) at 25°C with the  
303 parameterization given by Pérez and Fraga (1987b). The error in this potentiometric  
304 method was 0.010. In 2001, the seawater pH measurements were determined with a  
305 spectrophotometric method following Clayton and Byrne (1993), subsequently adding  
306 0.0047 to the pH value to do so (DelValls and Dickson, 1998). The precision of the  
307 spectrophotometric measurements was 0.003 pH units.

308

309 The pH values were reported on total pH scale at 0 dbar of pressure and both at 25°C  
310 and in situ temperature following the same procedure of GLODAP v2 (Olsen et al.,  
311 2019). A total of 12,220 measurements of pH on NBS scale were converted to the total  
312 scale using CO2SYS (Lewis and Wallace, 1998) for MATLAB (van Heuven et al.,  
313 2011) with pH and total alkalinity as inputs. The conversion was conducted with the  
314 carbonate dissociation constants of Lueker et al. (2000) and the borate-to-salinity ratio  
315 of Uppström (1974). Whenever total alkalinity data were missing, these values were  
316 approximated as 66 times salinity that is the mean ratio between the total alkalinity and  
317 the salinity of every in situ measurements compiled in the ARIOS database. Data for  
318 phosphate and silicate are also needed and were, whenever missing, a constant values of  
319  $10 \mu\text{mol kg}^{-1}$  for silicate and  $1 \mu\text{mol kg}^{-1}$  for phosphate were used. These  
320 approximations were tested on 8,296 samples with complete biogeochemical  
321 information showing a bias of less than 0.0004 pH units for 99.95% of the samples.

322

### 323 **Alkalinity measurements**

324 The seawater alkalinity was measured for the first time in 1981 by potentiometric  
325 titration with HCl 0.1 N at final pH 4.44 following Pérez and Fraga (1987a) with an  
326 analytical error of  $2 \mu\text{mol kg}^{-1}$  and a precision of 0.1%. Sodium tetraborate decahydrate  
327 (Borax,  $\text{Na}_2\text{B}_4\text{O}_7 \cdot 10\text{H}_2\text{O}$ , Merck p.a.) was used for standardizing the HCl (0.13 M). The  
328 pH measurements were carried out with a combined glass electrode (Metrohm E-121)  
329 with Ag/AgCl (KCl 3M) as the reference. The pH was calibrated using the NBS buffers  
330 assuming the theoretical slope. As of 2001, the accuracy of alkalinity measurements  
331 was determined using samples of certified reference material (CRM) provided by Dr. A.  
332 Dickson, University of California, improving the precision to  $\pm 1.4 \text{ mol kg}^{-1}$  and an  
333 accuracy of <0.1% recently established by (Ríos and Pérez, 1999) from cross-  
334 calculation with measured Certified Reference Materials (Dickson et al., 2007).

335



336 **Nutrient measurements**

337 Except in the campaigns called Galicia, where the samples were analysed on board, the  
338 samples collected are kept in the dark and cold (4°C) to be analysed in the laboratory.

339 Nutrient concentration was determined by a flow-segmented autoanalyzer (Technicon  
340 AAI and Alpkem after 1995) as described in Strickland and Parsons (1968) with the  
341 particularity that the reduction of nitrate to nitrite with Cd column is done using a citrate  
342 buffer according to Mouriño and Fraga's modification (1985). Phosphates and silicates  
343 were measured following Grasshoff (1983), and ammonium as described by Grasshoff  
344 and Johannsen (1972). This method was maintained in the subsequent cruises,  
345 achieving a precision of 0.02  $\mu\text{mol/kg}$  for nitrite, 0.1  $\mu\text{mol/kg}$  for nitrate, 0.05  $\mu\text{mol kg}^{-1}$   
346 for ammonium and silicate, and 0.01  $\mu\text{mol/kg}$  for phosphate.

347

348 **Oxygen measurements**

349 The dissolved oxygen was determined via the Winkler titration method for the first time  
350 in 1981 following the procedure published later by Culberson et al. (1991). The oxygen  
351 concentration in the samples in this method is fixed with  $\text{Cl}_2\text{Mn}$  and  $\text{NaOH/NaI}$ , which  
352 are kept in the dark until analysis in the laboratory 12-24 hours later. The measurements  
353 were made by titration of iodine with thiosulfate using an automatic titrator. During the  
354 80s and early 90s, the titration was carried out with Metrohm instruments (E-425 or E-  
355 473), which had an analytical error of 1  $\mu\text{mol kg}^{-1}$ . The oxygen concentration after 1997  
356 was estimated using a Titrino 720 (Metrohm) analyser with an accuracy of 0.5  $\mu\text{mol kg}^{-1}$ .  
357

358

359 **Chlorophyll measurements**

360 The chlorophyll-a values were measured following SCOR-UNESCO (1966) using a  
361 6 cm diameter Schleicher and Scholl 602eh filter covered with magnesium carbonate.  
362 The absorption was measured in 1 cm optical path cuvettes using a Beckman DU  
363 spectrophotometer. In 1984, discrete water samples of the chlorophyll-a samples were  
364 filtered through Whatman GF/C filters of 2.5 cm, which were preferred from then on,  
365 and measured fluorometrically following Strickland and Parsons (1972) without  
366 correction for concentration by pheophytes. The fluorescence readings were carried out  
367 with a Turner Designs 10,000 R fluorometer (Yentsh and Menzel, 1963) obtaining a  
368 precision of 0.05  $\text{g L}^{-1}$ .



369

### 370 **Quality control**

371 Every cruise gathered in the Table 1 passed 1<sup>st</sup> quality control to ensure truly confident  
372 results. The GO-SHIP software for quality control of hydrographic data (Velo et al.,  
373 2019) that compile several QC procedures was applied to ARIOS dataset. A quality flag  
374 was assigned to each measurement available from the repository sites (Table 2). This  
375 method was preferred over applying a very stringent flagging process because it is  
376 difficult to rule out some extreme values associated with low salinities or that could be  
377 supported by the high variability of an ecosystem with very high biological activity

378

379 The ARIOS database includes the cruise corrections for pH data of the -0.017 for the  
380 Galicia VIII cruise (29GD19840711) and +0.032 for Galicia IX cruise  
381 (29GD19860904) detected during the second level quality control of CARINA project  
382 (Velo et al., 2009).

383

### 384 **3.4. Distribution of sampling**

385 According to the type of region under study, different areas were identified in order to  
386 classify the measurements gathered in the oceanographic cruises (Fig. 1). The latitude  
387 of 43°N where Cape Finisterre is located was used as the dividing line between northern  
388 and southern waters. Subsequently, a criterion of depth also split the waters to the north  
389 of 43°N into north oceanic (below 250 m), north shelf (between 205 m and 75 m) and  
390 north coast (75 m to the surface). The southern shelf waters were divided by latitude  
391 42°N into Portuguese and the *Rías Baixas* (RB) shelves, whereas the shallower waters  
392 were identified by the main rias, where three different zones were defined using  
393 longitude boundaries (outer, middle and inner) according to Gago et al. (2003c) in the  
394 *Ría de Vigo*, and just two zones in the other rias (*Ría de Pontevedra*, *Ría de Arousa*, *Ría*  
395 *de Muros*). Southern waters between the isobath at 75 metres and the mouth of the  
396 estuaries were identified as the Portuguese and RB coast.

397

398 The discrete measurements gathered in the ARIOS dataset were mainly found in  
399 different regions' waters around 42°N latitude (Fig 1; Fig. 2a), especially in the outer  
400 and middle areas of the *Ría de Vigo*, which accounted for 15% and 21% of the total  
401 measurements respectively due to the proximity to the *Instituto de Investigaciones*  
402 *Mariñas* (IIM-CSIC). Most of the measurements (85%) carried out by many of these



403 cruises to study the coastal ecosystems concentrated on shallow waters between the  
404 seawater surface and 75 metres in depth (Fig. 2b). Although waters below 4,900 metres  
405 deep were also sampled, observations below 900 metres only account for 1% of the  
406 ARIOS database.

407

408 The observations made over more than 40 years in every region of the ARIOS database  
409 were irregular on both an interannual and seasonal scale (Fig. 2a). The period of most  
410 sampling activity was the 80s and 90s, whereas samples were especially scarce in the  
411 early 2010s. On a seasonal scale, summer and autumn were the preferred seasons to  
412 address the different research purposes, with 37% and 36% of the total samples  
413 respectively. The observations taken during less favourable winter conditions,  
414 especially aboard the coastal vessels usually available, only accounted for the 10% of  
415 the ARIOS database.

416

#### 417 **4. Results**

418 Some of the most obvious results provided by the ARIOS database are shown below.  
419 The purpose is to describe the environmental context and the main oceanographic  
420 processes that affect the variability of these discrete measurements and offer  
421 preliminary information for future detailed biogeochemical research.

422

##### 423 **4.1. Vertical distribution**

424 The vertical profile in the ocean region between 41°N and 43°N was estimated for each  
425 oceanographic station as the mean value of the depth ranges described in Figure 2b.  
426 These measurements were gathered attending to the collection periods (December-  
427 February, March-May, June-August and September-November) and averaged to  
428 describe winter, spring, summer and autumn respectively (Fig. 3).

429

430 The vertical distribution of the temperature (Fig. 3a) showed the presence of warmer  
431 saline waters throughout the water column in winter with the exception of the surface  
432 waters during summer, which showed intense heating due to the radiant solar energy.  
433 Below the maximum temperature observed during the summer, cold central waters of  
434 subpolar origin occupied the water columns with lower salinity (Fig. 3b). The vertical  
435 variation of temperature is typical for a temperate region with relatively homogenous  
436 deep water below the seasonal thermocline, reaching maximum SST values in summer



437 and autumn, and minimums in spring and winter. The winter temperature profile is  
438 relatively warmer than in spring because of the presence of the IPC (Alvarez-Salgado  
439 et al., 2006), which reaches a depth of 300 metres. The maximum salinity is also found in  
440 winter due to the presence of the IPC, whereas the minimum values are found in autumn  
441 (Fig. 3b). Below 500 metres in depth, the increase in salinity points to the presence of  
442 Mediterranean Water. These differences reach a minimum at 500 metres deep, where  
443 the salinity values coincided. From this depth to 1,100 metres, the differences in  
444 temperature and salinity throughout the four seasons were minimal, with the mean  
445 values converging to  $11.03 \pm 0.07^\circ\text{C}$  and  $36.117 \pm 0.009$  psu, respectively (Fig. 3ab).

446

447 The vertical distribution of pH,  $\text{NO}_3^-$  and oxygen concentration (Fig. 3cde) also showed  
448 a variation lower than 1% at this depth with annual means of  $15.2 \pm 0.1 \mu\text{mol kg}^{-1}$ ,  
449  $8.025 \pm 0.005$  and  $188 \pm 1 \mu\text{mol kg}^{-1}$  respectively. The pH values from a maximum  
450 subsurface located at around 40 metres deep showed a clear inverse correlation with the  
451 depth down to a depth of 500 metres throughout the seasonal cycle, where the annual  
452 minimum value of  $8.018 \pm 0.005$  was reached. The highest values were related to the  
453 biological  $\text{CO}_2$  drawdown, which brought the pH to a peak value of 8.13 at 40 metres  
454 deep during the spring bloom. Underneath this intense photosynthesis activity between  
455 the surface and 100 metres, the respiration of organic matter took the pH to lower  
456 values than those measured in winter between 200 to 500 metres, a depth at which the  
457 spring and winter values were practically equal. The impact on the growth of the  
458 phytoplankton community during the spring was also evident, judging by the oxygen  
459 concentration. So, in the upper waters the spring oxygen concentration values exceeded  
460 those of the winter values, while oxygen consumption was found from a depth of  
461 300 metres to 1,000 metres due to respiration from organic matter arriving from above.  
462 The minimum values for oxygen concentration throughout the water column were found  
463 during summer and autumn. The nitrate concentration displayed a particularly vertical  
464 distribution, growing with depth from minimum values in the upper layer of the ocean  
465 region, which was practically zero during the first 50 metres. Below 100 metres, the  
466 nitrate concentration showed the maximum values in the vertical distribution during  
467 summer and autumn coinciding with the presence of waters of subpolar and subtropical  
468 origin respectively, whereas the minimum values appeared in winter. Towards the  
469 bottom, the seasonal values of  $\text{NO}_3^-$  concentration were almost coincident at a mean



470 value of  $15.2 \pm 0.1 \mu\text{mol kg}^{-1}$ .

471

#### 472 **4.2. Seasonal cycle**

473 The seasonal cycle of the surface waters (0 to 5 metres) was estimated as a monthly  
474 filtered means, accepting only values within two standard deviations. Five regions that  
475 were located as a longitudinal transect between the inner *Ría de Vigo* and the ocean  
476 zone are shown in Fig. 4.

477

478 In general terms, the seasonal variability of the temperature was very similar in every  
479 area, ranging between 12 and 19°C (Fig. 4a). Only particular features observed on a  
480 short-term scale as in the examples below differ between each region. The warmer  
481 waters were usually found in the oceanic zone, reaching a maximum monthly averaged  
482 temperature of 18.6°C in September, while the coldest surface waters of 12.6°C were  
483 located in the inner stations closer to the mouth of the *Ría de Vigo* in January. Another  
484 secondary minimum averaged temperature was also found in the shelf and the outer area  
485 of the *Ría de Vigo*, which was remarkably low in August due to the entry of cold  
486 upwelled waters in the surface layer (Alvarez-Salgado 1993).

487

488 The monthly salinity averages (Fig. 4b) clearly showed significant differences between  
489 the offshore and coastal waters. Sharp salinity changes were seen in the estuary during  
490 winter, especially in the inner area where values lower than 28 psu were reached with  
491 the arrival of continental inputs in December. The weak seasonal cycle of salinity in the  
492 shelf and ocean waters showed high values in December due to the influence of warm  
493 saline water from the IPC, usually located on the shelf slope even though it may even  
494 enter the rias depending on the relative intensity of shelf winds and the intensity of the  
495 continental runoff (Alvarez-Salgado et al., 2003). In this sense, the slight salinity  
496 minimum observed in the shelf waters in March could be consequence of the offshore  
497 spreading of the maximum discharges from the River Miño and Douro (Otero et al.,  
498 2010) at the end of downwelling season. After this, the shelf and ocean waters showed  
499 minimum values in summer due to the arrival of cooler and fresher subpolar waters  
500 (Rios et al., 1992; Alvarez-Salgado et al., 2003, 2006). In August, coinciding with the  
501 maximum salinity of the surface waters in the interior of the *Ría de Vigo* due to the  
502 minimum river runoff, the surface waters between the inner *Ría de Vigo* and the ocean  
503 region were almost homogeneous, with minimum differences in salinity of 0.2 psu.



504

505 Like salinity, there was little seasonal variability in pH in the offshore waters, but large  
506 seasonable variability in coastal waters, with peak pH in spring and minimum pH in  
507 autumn in every region (Fig. 4c). The net balance between production and respiration of  
508 organic matter and the estuarine circulation caused a maximum pH of 8.19 in the outer  
509 region of the *Ría de Vigo* in May and a minimum of 7.96 in the inner waters in  
510 November.

511

512 The oxygen concentration (Fig. 4d) in the coastal ecosystems is also controlled by the  
513 remineralization of the organic matter and photosynthetic activity of the phytoplankton  
514 community, with the effect of salinity and temperature on the oxygen saturation level.  
515 The variability in the oxygen concentration, like the pH distribution, showed a growing  
516 seasonal amplitude towards the coastline, with maximum values in the outer and middle  
517 *Ría de Vigo* and lower values in the inner waters, especially during the second half of  
518 the seasonal cycle. Hence, the dissolved oxygen concentration mirrored the seasonal  
519 cycle of pH, showing growing seasonal amplitude towards the coastline with a range  
520 between  $284 \mu\text{mol kg}^{-1}$  found in the outer region of the *Ría de Vigo* in May and  $205$   
521  $\mu\text{mol kg}^{-1}$  in the inner waters in November. These results seem to reinforce the  
522 importance of the oxygen consumption in this shallow area, where the water column is  
523 less than 10 metres deep and so it would also be influenced by benthic respiration  
524 (Alonso-Pérez and Castro, 2014).

525

526 The monthly means of nitrate concentration (Fig. 4e) could be summarized as high  
527 values during autumn and winter due to the nutrients delivered from the continent and  
528 the vertical mixing, and as minimum nitrate values from March to September because of  
529 phytoplankton consumption. The nitrate concentration was markedly higher in the inner  
530 *Ría de Vigo*, where it exceeded  $9 \mu\text{mol kg}^{-1}$  in February and decreased towards the open  
531 ocean, where the highest monthly value was seen to be  $2.5 \mu\text{mol kg}^{-1}$ . Some notable  
532 aspects can be seen in Fig. 5d, such as water poor in nitrate in the ocean region between  
533 the two peaks of  $3.5 \mu\text{mol kg}^{-1}$  in March and  $1.3 \mu\text{mol kg}^{-1}$  in October. This shows the  
534 presence of the IPC waters, which are warmer and saltier than the shelf waters. Also  
535 noteworthy was the particular fact that while the nitrate concentration in other areas was  
536 practically zero in summer, the nitrate amount in the surface waters within the *Ría de*





537 *Vigo*, and especially in the inner *Ría de Vigo*, was not completely consumed. This  
538 indicates a constant supply throughout the year, either through upwelling events or the  
539 continental inputs. This in turn means that while the chlorophyll values were at a  
540 minimum in the offshore waters in summer, the phytoplankton community in the  
541 estuary grew in summer during the upwelling relaxation periods (Pérez et al., 2000).  
542 The nutrient concentration during spring and summer is only detectable in the recently  
543 upwelled waters. It can reach up to  $6 \mu\text{mol L}^{-1}$  (Fraga, 1981; Castro et al., 1994). During  
544 the cessation of the upwelling season in September and October, the chlorophyll  
545 concentration (Fig. 5f) rises again, sustained by nutrients entering from deeper waters  
546 through vertical mixing. It should be noted that there is a coincidence of high  
547 chlorophyll in the water column and low oxygen concentration in the inner *Ría de Vigo*  
548 from May to November, indicating the potential importance of benthic fluxes and  
549 vertical fluxes.

550

#### 551 **4.3. Long-term trend**

552 The long-term trends of these surface waters were estimated to be the interannual linear  
553 rate of the deseasonalized time series, previously removing the monthly means in these  
554 regions and assuming a null spatial variability. The significant trends in the ARIOS  
555 database, meaning long-term variability, should be interpreted as a combination of the  
556 natural variability on a decadal scale (Pérez et al., 2010; Padin et al., 2010) and  
557 anthropogenic forcings (Wolf-Gladrow et al., 1999; Anderson and Mackenzie 2004;  
558 Bakun et al., 2010).

559

560 No long-term temperature variability was found in the surface waters of any region  
561 despite the known warming previously reported on the Northern Iberian coast (Pérez et  
562 al., 2010; Gesteira et al., 2011; González-Pola et al., 2005). Unlike the temperature, the  
563 other expected consequence of climate change (Caldeira and Wickett, 2003), namely  
564 ocean acidification was observed along the longitudinal transect, with a greater decline  
565 in pH number towards the coast (Table 2). The long-term pH variation of -  
566  $0.0039 \pm 0.0005 \text{ yr}^{-1}$  in the inner waters was about triple the change of -  
567  $0.0012 \pm 0.0002 \text{ yr}^{-1}$  in the ocean zone, explaining the 34% and 22% variation in pH in  
568 situ respectively, and representing 1-3% of the seasonal pH variation in all zones. Other  
569 acidification rates estimated in different sites of the North Atlantic Ocean (Lauvset and  
570 Gruber, 2014; Bates et al., 2014) including  $-0.018 \text{ decade}^{-1}$  in the mean global ocean pH



571 (Lauvset et al., 2015) or  $-0.0164 \text{ decade}^{-1}$  in the Eastern North Atlantic by Ríos et al.  
572 (2001) are within the acidification range found in the ocean and coastal zones of these  
573 waters.

574

575 The long-term trend in salinity was also seen to be evidently dependent on the distance  
576 to the mouth of the ria. The interannual rate of sea surface salinity in the outer and inner  
577 *Ría de Vigo* previously reported by Rosón et al. (2009) was  $0.0426 \pm 0.016 \text{ psu yr}^{-1}$  and  
578  $0.0193 \pm 0.0056 \text{ psu yr}^{-1}$  respectively. These changes were observed in parallel to an  
579 interannual alkalinity increase that is cancelled out in the normalized alkalinity,  
580 estimated as the difference between the alkalinity measured and the alkalinity calculated  
581 using the linear regression with salinity in each region. So, the interannual salinity  
582 increase was the forcing that explains the increase in the buffer capacity of the surface  
583 waters (Sarmiento and Gruber, 2006).

584

585 Other significant long-term variations were found in other biogeochemical parameters  
586 in the ARIOS database. The long-term trend of the nutrient concentration in the inner  
587 *Ría de Vigo* showed an increase in the nitrate, phosphate and ammonium concentrations  
588 of  $0.0158 \pm 0.006 \text{ } \mu\text{mol kg}^{-1} \text{ yr}^{-1}$ ,  $0.0076 \pm 0.0016 \text{ } \mu\text{mol kg}^{-1} \text{ yr}^{-1}$  and  
589  $0.0560 \pm 0.0011 \text{ } \mu\text{mol kg}^{-1} \text{ yr}^{-1}$  respectively (Doval et al., 2016). This fertilization on a  
590 long-term scale in the surface waters of the inner ria was observed in parallel to the  
591 deoxygenation of  $-0.7 \pm 0.2 \text{ } \mu\text{mol kg}^{-1} \text{ yr}^{-1}$ . The apparent oxygen utilisation (AOU),  
592 calculated using the concentration of  $\text{O}_2$  at saturation calculated according to Benson  
593 and Krause (1984), underwent an equivalent significant long-term change of  
594  $0.7 \pm 0.2 \text{ } \mu\text{mol kg}^{-1} \text{ yr}^{-1}$ , indicating that either the biological consumption rates, or a  
595 change in the amount of time that the waters are ventilated, or even its interaction or  
596 exchange with the sediment, cause the the long-term reduction of oxygen. .

597

598 Attending to the interannual salinity changes in the shallower waters of the *Ría de Vigo*,  
599 these findings seem to be related to a weakening of the vertical salinity gradient and a  
600 growing exchange between the bottom and surface waters. So, the footprint of oxygen  
601 consumption and the remineralized nutrient inputs resulting from benthic respiration  
602 seem to reach the upper layer. The metabolic processes in a more homogeneous water  
603 column would also explain an intense acidification in the inner waters in spite of  
604 growing alkalinity buffering.



605

606 The mean values at each station of the ARIOS database estimated for each depth range  
607 described in Figure 2, resulting in 8,384 values, were used to estimate a general value of  
608 the long-term trend in pH. The historical pH values in situ from the ARIOS database  
609 showed a general decrease in seawater pH in the Iberian Upwelling between 1976 and  
610 2018, with an acidification rate of  $-0.012 \pm 0.002 \text{ yr}^{-1}$  that significantly explains 2% of  
611 the total pH variation (Fig. 5a). The apparent oxygen utilisation was also shown as  
612 function of pH over time, revealing the association of higher AOU values with lower  
613 pH. The relationship between pH and AOU (Fig. 5b) showed an inverse linear  
614 correlation of  $-399 \pm 5 \mu\text{mol kg}^{-1}$ . The strong biological activity of the upwelling systems  
615 is the main driver of pH changes, explaining 52% of the observed variation in the  
616 discrete measurements. The distribution of nitrate seen in relation to the distribution of  
617 pH and AOU (Fig. 5b) showed the association of higher pH values with negative AOU  
618 values and a nitrate decrease, reinforcing the importance of biological processes in  
619 these marine carbonate system.

620

621 Although the different processes controlling the AOU values were not separated in this  
622 analysis, the oxygen concentration in addition to the remineralization and  
623 photosynthesis of organic matter is conditioned by changes in temperature and salinity,  
624 ventilation events, water masses mixing and other processes (Sarmiento and Gruber,  
625 2006). Therefore, the long-term drop in seawater pH measurements in this region  
626 responding to the intrusion of atmospheric  $\text{CO}_2$  may also be due to the impact of other  
627 interannual changes affecting the seawater pH, such as biological activity. So, the future  
628 evolution of acidification will respond both to the potential increase in  $\text{CO}_2$  in the  
629 atmosphere and to other long-term changes affecting the seawater's carbonate system.

630

### 631 **5. Data availability**

632 The ARIOS dataset (Pérez et al., 2020) is archived at DIGICAL CSIC under the Digital  
633 Object Identifier (DOI): <http://dx.doi.org/10.20350/digitalCSIC/12498>.

634

635 The data are available as WHP-Exchange bottle format (arios\_database\_hy1.csv). A  
636 documentation file (readme\_ARIOSDATABASE.txt) provides an description of the  
637 material and methods of the measurements and the parameters of the dataset. In both  
638 files, a table similar to the Table 1 of this manuscript include the DOI and the



639 EXPCODE of the original cruise files gathered in the ARIOS dataset.

640

641 These data are available to the public and the scientific community with the aim of that  
642 their wide dissemination will lead to new scientific knowledge about the ocean  
643 acidification and the biogeochemistry of the Galicia Upwelling System. The dataset is  
644 subject to a Creative Commons License Attribution-ShareAlike 4.0 International  
645 (<http://creativecommons.org/licenses/by-sa/4.0/>) and users of the ARIOS dataset should  
646 reference this work.

647

## 648 **6. Conclusions**

649 The ARIOS database is a unique compilation of biogeochemical discrete measurements  
650 in the Iberian Upwelling Ecosystem from 1976 to 2018. This data set comprises more  
651 than 17,653 discrete samples from 3,357 oceanographic stations (but not always for all  
652 parameters) of pH, alkalinity and associated physical and biogeochemical parameters  
653 (e.g., temperature, salinity, and chlorophyll and oxygen concentrations). The material  
654 and methods varied throughout the sampling period due to logistical and analytical  
655 issues such as those described in Table 1, where different sites are mentioned to  
656 download these measurements and detailed information.

657

658 Among the results described as preliminary and relevant information to learn the  
659 environmental and oceanographic context of the ARIOS database, we can mention the  
660 following main points concerning the pH characteristics of the Iberian Upwelling  
661 System:

- 662 • A decrease in seawater pH in the Iberian Upwelling between 1976 and 2018,  
663 with an acidification rate of  $-0.012 \pm 0.002 \text{ yr}^{-1}$  that significantly explains 2% of  
664 the total pH variation
- 665 • An interannual pH variation of  $-0.0039 \pm 0.0005 \text{ yr}^{-1}$  in the inner waters and -  
666  $0.0012 \pm 0.0002 \text{ yr}^{-1}$  in the ocean zone.
- 667 • An inverse linear correlation between pH and AOU of  $-399 \pm 5 \mu\text{mol kg}^{-1}$  that  
668 explained 52% of the observed variation in the discrete measurements.

669

670 This published ARIOS database is a useful and necessary tool to confirm and study  
671 biogeochemical changes in the seawater at long term trend. Likewise, we understand  
672 that it is a starting point to which to add future observation projects to continue



673 increasing the knowledge about the impact of climate change in the Iberian Upwelling  
674 Ecosystem.

675

#### 676 **Acknowledgements.**

677 The compilation of this data set was funded by the ARIOS project (CTM2016-76146-  
678 C3-1-R) funded by the Spanish government through the Ministerio de Economía y  
679 Competitividad that included European FEDER funds. Part of the processing work was  
680 supported by the MarRISK project (European Union FEDER 0262\_MarRISK\_1\_E)  
681 funded by the Galicia-Northern Portugal Cross-Border Cooperation Program  
682 (POCTEP). This project has also received funding from the European Union's Horizon  
683 2020 research and innovation programme under grant agreement No 820989 (project  
684 COMFORT, Our common future ocean in the Earth system – quantifying coupled  
685 cycles of carbon, oxygen, and nutrients for determining and achieving safe operating  
686 spaces with respect to tipping points). This data set encompasses decades of work  
687 conducted by an overwhelming number of people. We thank all of the scientists,  
688 technicians, personnel, and crew who were responsible for the collection and analysis of  
689 the over 22 000 samples included in the final data set. In addition to the PI cited in  
690 Table 1 we also thank to Trinidad Rellán, Antón Velo, Miguel Gil Coto, Marta Alvarez,  
691 Marylo Doval, Jesus Gago, Daniel Broullón and Marcos Fontela. We also thank Monica  
692 Castaño for starting this data compilation more than 10 years ago.

693

#### 694 **References**

695 Alonso-Perez F., Ysebaert, T., and Castro, C. G.: Effects of suspended mussel culture  
696 on benthic-pelagic coupling in a coastal upwelling system (Ría de Vigo, NW Iberian  
697 Peninsula), *Journal of Experimental Marine Biology and Ecology*, 382–391,  
698 <https://doi.org/10.1016/j.jembe.2009.11.008>, 2010.

699

700 Alonso-Perez, F., and Castro, C. G.: Benthic oxygen and nutrient fluxes in a coastal  
701 upwelling system (Ría de Vigo, NW Iberian Peninsula): seasonal trends and regulating  
702 factors. *Mar Ecol Prog Ser* 511:17-32. <https://doi.org/10.3354/meps10915>. 2014.

703

704 Alonso-Perez, F., Zúñiga, D., Arbones, B., Figueiras, F. G., and Castro, C. G.: Benthic  
705 fluxes, net ecosystem metabolism and seafood harvest: Completing the organic carbon



- 706 balance in the Ría de Vigo (NW Spain), *Estuarine Coastal Shelf Science*, 163,  
707 <https://doi.org/10.1016/j.ecss.2015.05.038>. 2015.
- 708
- 709 Alvarez-Salgado, X. A., Rosón, G., Pérez, F. F. and Pazos, Y.: Hydrographic variability  
710 off the Rías Baixas (NW Spain) during the upwelling season. *Journal of Geophysical*  
711 *Research* 98, 14447–14455, 1993.
- 712
- 713 Alvarez-Salgado, X. A., Figueiras, F. G., Villarino, M. L., and Pazos, Y.:  
714 Hydrodynamic and chemical conditions during onset of a red-tide assemblage in an  
715 estuarine upwelling ecosystem, *Marine Biology*, 130, 509–519, 1998.
- 716
- 717 Alvarez, M., Fernández, E., and Pérez, F. F.: Air-sea CO<sub>2</sub> fluxes in a coastal embayment  
718 affected by upwelling: physical versus biological control, *Oceanologica Acta*, 22, 5,  
719 499–515, 1999.
- 720
- 721 Álvarez-Salgado, X. A., Doval, M.D., Borges, A.V, Joint, I., Frankignoulle, M.,  
722 Woodward, E.M.S., and Figueiras, F.G.: Off-shelf fluxes of labile materials by an  
723 upwelling filament in the NW Iberian Upwelling System, *Prog. Oceanogr.*, 51(2–4),  
724 321–337, 2001.
- 725
- 726 Álvarez-Salgado, X. A., Beloso, X., Joint, I., Nogueira, E., Chou, L., Pérez, F. F.,  
727 Groom, S., Cabanas, J. M., Rees, A.P., and Elskens, M.: New Production of the NW  
728 Iberian Shelf during the Upwelling Season over the period 1982-1999. *Deep-Sea Res.*  
729 49(10), [http://dx.doi.org/10.1016/S0967-0637\(02\)00094-8](http://dx.doi.org/10.1016/S0967-0637(02)00094-8), 2002.
- 730
- 731 Álvarez-Salgado, X. A., Figueiras, F. G., Pérez, F. F., Groom, S., Nogueira, E., Borges,  
732 A. V., Chou, L., Castro, C. G., Moncoiffé, G., Ríos, A. F., Miller, A.E.J., Frankignoulle,  
733 M., Savidge, G., and Wollast, R.: The Portugal coastal counter current off NW Spain  
734 new insights on its biogeochemical variability, *Progress in Oceanography*, 56(2)  
735 [http://dx.doi.org/10.1016/S0079-6611\(03\)00007-7](http://dx.doi.org/10.1016/S0079-6611(03)00007-7), 2003.
- 736
- 737 Álvarez-Salgado, X. A., Nieto-Cid, M., Piedracoba, S., Crespo, B. G., Gago, J., Brea,  
738 S., Teixeira, I. G., Figueiras, F. G., Garrido, J. L., Rosón, G., Castro, C. G., and Gilcoto,  
739 M.: Origin and fate of a bloom of *Skeletonema costatum* during a winter



740 upwelling/downwelling sequence in the Ría de Vigo (NW Spain), *Journal of Marine*  
741 *Research*, 63, 6, 1127–1149, <http://dx.doi.org/10.1357/002224005775247616>, 2005.

742

743 Alvarez-Salgado, X. A., Nieto-Cid, M., Gago, J., Brea, S., Castro, C. G., Doval, M., and  
744 Pérez, F. F.: Stoichiometry of the degradation of dissolved and particulate biogenic  
745 organic matter in the NW Iberian upwelling, *Journal of Geophysical Research*, 111,  
746 C07017, <http://dx.doi.org/10.1029/2004JC002473>, 2006.

747

748 Anderson, L.: Correction of reversing thermometers and related depth calculations in  
749 Baltic water, *Meddelande fran Havsfiskelaboratoriet*. Lysekil, 166, 1974.

750

751 Andersson, A. J., and Mackenzie, F. T.: Revisiting four scientific debates in ocean  
752 acidification research, *Biogeosciences*, 9, 893–905, [www.biogeosciences.net/9/893/2012/](http://www.biogeosciences.net/9/893/2012/),  
753 2012.

754

755 Arístegui J., Barton, E. D., Tett, P., Montero, M. F., García-Muñoz, M., Basterretxea,  
756 G., Cussatlegras, A. S., Ojeda, A., and de Armas, D.: Variability in plankton community  
757 structure, metabolism, and vertical carbon fluxes along an upwelling filament (Cape  
758 Juby, NW Africa), *Prog. Oceanogr.*, 62 (2-4), 95–113, 2004.

759

760 Bakun, A., Field, D. B., Redondo-Rodriguez, A., and Weeks, S. J.: Greenhouse gas,  
761 upwelling favorable winds, and the future of coastal ocean upwelling ecosystems.  
762 *Global Change Biology*, 16, 4, 1213–1228, [https://doi.org/10.1111/j.1365-](https://doi.org/10.1111/j.1365-2486.2009.02094.x)  
763 [2486.2009.02094.x](https://doi.org/10.1111/j.1365-2486.2009.02094.x), 2010.

764

765 Barnes, H.: *Apparatus and methods of oceanography*. Part one: Chemical, Allen and  
766 Unwin. London, 335 p., 1959.

767

768 Barton, E. D., Largier, J. L., Torres, R., Sheridan, M., Trasviña, A., Souza A., Pazos,  
769 Y., and Valle-Levinson, A.: Coastal upwelling and downwelling forcing of circulation  
770 in a semi-enclosed bay: Ria de Vigo, *Progress in Oceanography*, 134, 173–189.  
771 <https://doi.org/10.1016/j.pocean.2015.01.014>, 2015.

772



773 Barton, E. D., Torres, R., Figueiras, F. G., Gilcoto, M., and Largier, J.: Surface water  
774 subduction during a downwelling event in a semienclosed bay, *Journal Geophys.*  
775 *Research*, 121, 7088–7107, <https://doi.org/10.1002/2016JC011950>, 2016.

776

777 Barton, E. D., Castro, C. G., Alonso-Pérez, F., Zúñiga, D., Rellán, T., Arbones, B.,  
778 Castaño, M., Gilcoto, M., Torres, R., Figueiras, F. G., Pérez, F. F. and Ríos, A. F.: Cria  
779 surveys: hydrographic and chemical data, Digital.CSIC,  
780 <http://dx.doi.org/10.20350/digitalCSIC/9931>, 2019.

781

782 Bates, N. R., Astor, Y. M., Church, M. J., Currie, K., Dore, J. E., González-Dávila, M.,  
783 Lorenzoni, L., Muller-Karger, F., Olafsson, J., and Santana-Casiano, J. M.: A Time-  
784 Series View of Changing Surface Ocean Chemistry Due to Ocean Uptake of  
785 Anthropogenic CO<sub>2</sub> and Ocean Acidification, *Oceanography*, 27, 1, SPECIAL ISSUE  
786 ON Changing Ocean Chemistry, pp. 126–141, Published by: Oceanography Society  
787 <https://www.jstor.org/stable/24862128>. 2014.

788

789 Benson, B. B., and Krause, D. J.: The concentration and isotopic fractionation of  
790 oxygen dissolved in fresh water and seawater in equilibrium with the atmosphere.  
791 *Limnology and Oceanography*, 29(3), 620–632, 1984.

792

793 Blanton, J. O., Atkinson, L. P., Fernandez de Castillejo, F., and Lavin Montero, A.:  
794 Coastal upwelling off the Rias Bajas, Galicia, Northwest Spain, I: Hydrography studies.  
795 *Rapports et Proc-verbeaux Reun. Cons. into Explor. Mer*, 183, 79–90, 1984.

796

797 Bode, A., Alvarez-Ossorio, M. T., Cabanas, J. M.: Miranda, A., Varela, M.: Recent  
798 trends in plankton and upwelling intensity off Galicia (NW Spain), *Progress in*  
799 *Oceanography*, 83, 342–350, 2009.

800

801 Caldeira, K., and Wickett, M.E.: Oceanography: anthropogenic carbon and ocean  
802 pH, *Nature*, 425, 365, <https://doi.org/10.1038/425365a>, 2003.

803

804 Castro, C. G., Pérez, F. F., Álvarez-Salgado, X. A., Rosón, G., and Ríos, A. F.:  
805 Hydrographic conditions associated with the relaxation of an upwelling event off the





- 806 Galician coast (NW Spain), *Journal of Geophysical Research*, 99, C3, 5135–5147,  
807 <https://agupubs.onlinelibrary.wiley.com/doi/10.1029/93JC02735>, 1994.  
808
- 809 Castro, C. G., Nieto-Cid, M., Álvarez-Salgado, X. A., and Pérez, F. F.: Local  
810 remineralization patterns in the mesopelagic zone of the ENAW, *Deep Sea Research*  
811 Part I, 53 (12), 1925–1940, <http://dx.doi.org/10.1016/j.dsr.2006.09.002>, 2006.  
812
- 813 Castro, C. G., Álvarez-Salgado, X. A., Nogueira, E., Gago, J., Pérez, F. F., Bode, A.,  
814 Ríos, A. F., Rosón, G., and Varela, M.: Evidencias bioquímicas do cambio  
815 climático. Edita: Xunta de Galicia. Consellería de Medio Ambiente e Desenvolvemento  
816 Sostible, *Evidencias e impactos do cambio climático en Galicia*, 303–326, 2009.  
817
- 818 Clayton, T. D., and Byrne, R. H.: Spectrophotometric seawater pH measurements: total  
819 hydrogen ion concentration scale calibration of m-cresol purple and at-sea results, *Deep*  
820 *Sea Research I*, 40, 10, 2115–2129, [https://doi.org/10.1016/0967-0637\(93\)90048-8](https://doi.org/10.1016/0967-0637(93)90048-8),  
821 1993.  
822
- 823 Cobo-Viveros, A. M., Padin, X. A., Otero, P., de la Paz, M., Ruiz-Villareal, M., Ríos,  
824 A. F., Pérez, F. F.: Short-term variability of surface carbon dioxide and sea-air CO<sub>2</sub>  
825 fluxes in the shelf waters of the Galician coastal upwelling system, *Scientia Marina*,  
826 77S1, doi: 10.3989/scimar.03733.27C, 2013.  
827
- 828 Culberson, C. H., Knapp, G., Stalcup, M. C., Williams, R. T., and Zemlyak, F.: A  
829 comparison of methods for the determination of dissolved oxygen in seawater. WOCE  
830 Report 73/91, 77 pp, 1991.  
831
- 832 DelValls, T. A., and Dickson, A. G.: The pH of buffers based on 2-amino-2-  
833 hydroxymethyl-1,3-propanediol (“tris”) in synthetic sea water, *Deep-Sea Res. I*, 45,  
834 1541–1554, 1998.  
835
- 836 Dickson, A.G., Sabine, C.L., and Christian, J.R.: Guide to best practices for ocean CO<sub>2</sub>  
837 measurements. PICES Special Publication 3, 191 pp, 2007.  
838



- 839 Doval, M., Nogueira, E., and Pérez, F. F.: Spatio-temporal variability of the  
840 thermohaline and biogeochemical properties and dissolved organic carbon in a coastal  
841 embayment affected by upwelling: the Ría de Vigo (NW Spain). *Journal of Marine*  
842 *Systems*, 14, 1-2, 135–150, [https://doi.org/10.1016/S0924-7963\(97\)80256-4](https://doi.org/10.1016/S0924-7963(97)80256-4), 1998.
- 843
- 844 Doval, M. D., Alvarez-Salgado, X. A., and Perez, F. F.: Dissolved organic carbon in a  
845 temperate embayment affected by coastal upwelling, *Mar. Ecol. Prog. Ser.*, 157, 21–37,  
846 doi:10.3354/meps157021, 1997a.
- 847
- 848 Doval, M. D., Fraga, F. and Perez, F.F.: Determination of dissolved organic nitrogen in  
849 seawater using Kjeldahl digestion after inorganic nitrogen removal, *Oceanol. Acta.*  
850 <https://archimer.ifremer.fr/doc/00093/20429/18096.pdf>, 1997b.
- 851
- 852 Doval, M.D., López, A., and Madriñán, M.: Temporal variation and trends of inorganic  
853 nutrients in the coastal upwelling of the NW Spain (Atlantic Galician rías),  
854 *Journal of Sea Research*, 108, 19–29, <https://doi.org/10.1016/j.seares.2015.12.006>,  
855 2016.
- 856
- 857 Fraga F.: Upwelling off the Galician coast, northwest Spain. *Coastal Upwelling*,  
858 American Geophysical Union, Washington DC, pp. 176–182,  
859 <https://doi.org/10.1029/CO001p0176>, 1981.
- 860
- 861 Fraga, F., Mouriño, C., and Manriquez, M.: Las masas de agua en la costa de Galicia:  
862 junio-octubre. *Result. Exped. Cient. Supl. Invest. Pesq.*, 10, 51–77,  
863 <http://hdl.handle.net/10261/90380>, 1982.
- 864
- 865 Fraga, F., Pérez, F. F., Figueiras, F. G., and Ríos, A. F.: Stoichiometric variations of N,  
866 P, C and O<sub>2</sub> during a *Gymnodinium catenatum* red tide and their interpretation, *Marine*  
867 *Ecology Progress Series*, 87, 1-2, 123–134, doi:10.3354/meps087123, 1992.
- 868
- 869 Figueiras, F. G., Jones, K., Mosquera, A. M., Álvarez Salgado, X. A., Edwards, A. and  
870 MacDougall, N.: Red tide assemblage formation in an estuarine upwelling ecosystem:  
871 Ria de Vigo, *Journal of Plankton Research*, 16 (7), 857–878,  
872 <https://doi.org/10.1093/plankt/16.7.857>, 1994.



873

874 Froján, M., Arbones, B., Zúñiga, D., Castro, C. G., and Figueiras, F. G.: Microbial  
875 plankton community in the Ría de Vigo (NW Iberian upwelling system): impact of the  
876 culture of *Mytilus galloprovincialis*, *Mar Ecol Prog Ser*, 498, 43–54,  
877 <https://doi.org/10.3354/meps10612>, 2014.

878

879 Froján, M., Figueiras, F. G., Zúñiga, D., Alonso-Pérez, F., Arbones, B., and Castro, C.  
880 G.: Influence of Mussel Culture on the Vertical Export of Phytoplankton Carbon in a  
881 Coastal Upwelling Embayment (Ría de Vigo, NW Iberia), *Estuaries and Coasts*, 39,  
882 1449–1462, <https://doi.org/10.1007/s12237-016-0093-1>, 2016.

883

884 Froján, M., Castro, C. G., Zúñiga, D., Arbones, A., Alonso-Pérez, F., and Figueiras, F.  
885 G.: Mussel farming impact on pelagic production and respiration rates in a coastal  
886 upwelling embayment (Ría de Vigo, NW Spain), *Estuarine, Coastal and Shelf Science*,  
887 204, 130–139, <https://doi.org/10.1016/j.ecss.2018.02.025>, 2018.

888

889 Frouin, R., Fiúza, A. F. G., Ambar, I., and Boyd, T. J. \_: Observations of a poleward  
890 surface current off the coasts of Portugal and Spain during winter, *Journal of*  
891 *Geophysical Research*, 95, 679–691, 1990.

892

893 Feely, R. A., Sabine, C. L., Hernandez-Ayon, J. M., Ianson, D., and Hales, B: Evidence  
894 for upwelling of corrosive “acidified” water onto the continental shelf, *Science*  
895 320(5882), 1490–1492, doi:10.1126/science.1155676, 2008.

896

897 Gago, J., Alvarez-Salgado, X. A., Gilcoto, M., and Pérez, F. F.: Assessing the  
898 contrasting fate of dissolved and suspended organic carbon in a coastal upwelling  
899 system (Ría de Vigo, NW Iberian Peninsula), *Estuarine, Coastal and Shelf Science*, 56,  
900 2, 271–279, [http://dx.doi.org/10.1016/S0272-7714\(02\)00186-5](http://dx.doi.org/10.1016/S0272-7714(02)00186-5), 2003a.

901

902 Gago, J., Alvarez-Salgado, X. A., Pérez, F. F., and Ríos, A. F.: Partitioning of physical  
903 and biogeochemical contributions to short-term variability of pCO<sub>2</sub> in a coastal  
904 upwelling system a quantitative approach, *Marine Ecology Progress*, 255, 43–54,  
905 <http://dx.doi.org/10.3354/meps25504>, 2003b.

906



907 Gago, J., Gilcoto, M., Pérez, F. F., and Ríos, A.F.: Short-term variability of fCO<sub>2</sub> in  
908 seawater and air-sea CO<sub>2</sub> fluxes, *Marine Chemistry*, 80, 4, 247–264,  
909 [http://dx.doi.org/10.1016/S0304-4203\(02\)00117-2](http://dx.doi.org/10.1016/S0304-4203(02)00117-2), 2003c.

910

911 Gilcoto, M., Largier, J. L., Barton, E. D., Piedracoba, S., Torres, R., Graña, R., Alonso-  
912 Pérez, F., Villaceros-Robineau, N., and de la Granda, F.: Rapid response to coastal  
913 upwelling in a semienclosed bay, *Geophysical Research Letters*, 44(5), 2388–2397, doi:  
914 10.1002/2016GL072416, 2017.

915

916 González-Pola, C., Lavín, A., Vargas-Yáñez, M.: Intense warming and salinity  
917 modification of intermediate water masses in the southeastern corner of the Bay of  
918 Biscay for the period 1992–2003, *Journal of Geophysical Research*, 110, C05020,  
919 doi:10.1029/2004JC002367, 2005.

920

921 Grasshoff, K., Johannsen, H.: A New Sensitive and Direct Method for the Automatic  
922 Determination of Ammonia in Sea Water, *ICES Journal of Marine Science*, 34(3), 516–  
923 521, <https://doi.org/10.1093/icesjms/34.3.516>, 1972.

924

925 Grasshoff, K., Ehrhardt, M., Kremling, K.: *Methods of Seawater Analysis*, 2nd. ed.  
926 Verlag Chemie, Weinheim, 419 pp, 1983.

927

928 Gruber, N., Hauri, C., Lachkar, Z., Loher, D., Frolicher, T. L., and Plattner, G. K.:  
929 Rapid progression of ocean acidification in the California Current System, *Science*, 337,  
930 220–223, doi:10.1126/science.1216773, 2012.

931

932 Hauri, C., Gruber, N., Plattner, G. K., Alin, S., Feely, R. A., Hales, B., and Wheeler,  
933 P. A.: Ocean acidification in the California Current System, *Oceanography*, 22, 58–69,  
934 doi:10.5670/oceanog.2009.97, 2009.

935

936 Hauri, C., Gruber, N., Vogt, M. S., Doney, C., Feely, R. A., Lachkar, Z., Leinweber, A.,  
937 McDonnell, A. M. P., Munnich, M., and Plattner, G.K.: Spatiotemporal variability and  
938 long-term trends of ocean acidification in the California Current System,  
939 *Biogeosciences*, 10, 193–216, doi:10.5194/bg-10-193-2013, 2013.



- 940 Hofmann, G. E.: High-frequency dynamics of ocean pH: A multi-ecosystem  
941 comparison, *PLoS One*, 6(12), e28983, doi:10.1371/journal.pone.0028983, 2011.  
942
- 943 IPCC: Climate Change 2013: the physical science basis Contribution of Working Group  
944 I to the Fifth Assessment Report of the Intergovernmental Panel on Climate Change ed  
945 T F Stocker et al (Cambridge: Cambridge University Press) pp 1535,  
946 www.ipcc.ch/report/ar5/wg1/, 2013.  
947
- 948 Lachkar, Z.: Effects of upwelling increase on ocean acidification in the California and  
949 Canary Current systems, *Geophys. Res. Lett.*, 41, 90–95, doi:10.1002/2013GL058726,  
950 2014.  
951
- 952 Lassoued, J., Babarro, J., Padín, X. A., Comeau, L., Bejaoui, N., and Pérez, F.:  
953 Behavioural and eco-physiological responses of the mussel *Mytilus galloprovincialis*  
954 to acidification and distinct feeding regimes, *Marine Ecology Progress Series*, 626, 97–  
955 108, doi: 10.3354/meps13075, 2019.  
956
- 957 Lauvset, S.K., and Gruber, N.: Long-term trends in surface ocean pH in the North  
958 Atlantic, *Marine Chemistry*, 162, 71–76,  
959 https://doi.org/10.1016/j.marchem.2014.03.009, 2014.  
960
- 961 Lauvset, S. K., Gruber, N., Landschützer, P., Olsen, A., and Tjiputra, J.: Trends and  
962 drivers in global surface ocean pH over the past 3 decades, *Biogeosciences*, 12(5),  
963 1285–1298, doi:10.5194/bg-12-1285-2015, 2015.  
964
- 965 Lewis, E., Wallace, D.W.R.: Program developed for CO<sub>2</sub> system calculations,  
966 ORNL/CDIAC-105, Carbon Dioxide Information Analysis Center, Oak Ridge National  
967 Laboratory, Oak Ridge, TN, USA, 1998.  
968
- 969 Lemos, R. T., and Sansó, B.: Spatio-temporal variability of ocean temperature in  
970 the Portugal Current System, *Journal of Geophysical Research*, 111, C04010,  
971 doi:10.1029/2005JC003051, 2006.  
972



- 973 Lueker, T. J., Dickson, A. G., and Keeling, C. D.: Ocean pCO<sub>2</sub> calculated from  
974 dissolved inorganic carbon, alkalinity, and equations for K-1 and K-2: validation based  
975 on laboratory measurements of CO<sub>2</sub> in gas and seawater at equilibrium, *Mar. Chem.*,  
976 70, 105–119, 2000.  
977
- 978 McElhany, P. and Shallin Busch, D.: Appropriate pCO<sub>2</sub> treatments in ocean  
979 acidification experiments, *Marine Biology*, 160, 1807–1812,  
980 <https://doi.org/10.1007/s00227-012-2052-0>, 2013.  
981
- 982 Mehrbach, C., Culberson, C. H., Hawley, J. E., and Pytlowicz, R. M.: Measurements of  
983 the apparent dissociation constant of carbonic acid in seawater at atmospheric pressure,  
984 *Limnology and Oceanography*, 18, 897–907, 1973.  
985
- 986 Miguez, B. M., Fariña-Busto, L., Figueiras, F. G., Pérez, F. F.: Succession of  
987 phytoplankton assemblages in relation to estuarine hydrodynamics in the Ria de Vigo,  
988 *Scientia Marina*, 65, S1, <https://doi.org/10.3989/scimar.2001.65s165>, 2001.  
989
- 990 Mouriño, C., and Fraga, F.: Determinación de nitratos en agua de mar, *Investigaciones*  
991 *Marinas*, 49 (1), 81–96, 1985.  
992
- 993 Nieto-Cid, M., Alvarez-Salgado, X. A., Brea, S., and Pérez, F. F.: Cycling of dissolved  
994 and particulate carbohydrates in a coastal upwelling system (NW Iberian Peninsula),  
995 [doi:10.3354/meps283039](https://doi.org/10.3354/meps283039), 2004.  
996
- 997 Nieto-Cid, M., Alvarez-Salgado, X. A., and Pérez, F. F.: Microbial and photochemical  
998 reactivity of fluorescent dissolved organic matter in a coastal upwelling system  
999 <https://doi.org/10.4319/lo.2006.51.3.1391>, 2006.  
1000
- 1001 Nogueira, E., Pérez, F. F., and Ríos, A. F.: Seasonal and long-term trends in an  
1002 estuarine upwelling ecosystem (Ría de Vigo, NW Spain), *Estuarine, Coastal and Shelf*  
1003 *Science* 44, 285–300, 1997.  
1004



- 1005 Olsen, A., Lange, N., Key, R. M., Tanhua, T., Álvarez, M., Becker, S., et al.:  
1006 GLODAPv2.2019: An update of GLODAPv2. *Earth System Science Data*, 11(3), 1437-  
1007 1461. <https://doi.org/10.5194/essd-11-437-2019>, 2019.  
1008  
1009 Orr, F. M.: Onshore Geologic Storage of CO<sub>2</sub>, *Science*, 25, 325, 1656–1658, doi:  
1010 10.1126/science.1175677, 2009.  
1011  
1012 Otero, P., Ruiz-Villarreal, M., and Peliz, A.: Variability of river plumes off Northwest  
1013 Iberia in response to wind events, *Journal of Marine Systems*, 72(1-4), 238–255, 2008.  
1014  
1015 Padin X. A., Castro, C. G., Ríos, A.F., and Pérez, F.F.: Oceanic CO<sub>2</sub> uptake and  
1016 biogeochemical variability during the formation of the Eastern North Atlantic Central  
1017 water under two contrasting NAO scenarios, *Journal of Marine Systems*, 84, 3-4, 96–  
1018 105, <https://doi.org/10.1016/j.jmarsys.2010.10.002>, 2010.  
1019  
1020 Pauly, D., and Christensen, V.: Primary production required to sustain global fisheries,  
1021 *Nature*, 374(6519), 255–257, 1995.  
1022  
1023 Pérez, F. F., and Fraga, F.: A precise and rapid analytical procedure for alkalinity  
1024 determination, *Marine Chemistry*, 21, 169–182, 1987a.  
1025  
1026 Pérez, F. F., and Fraga, F.: The pH measurements, in seawater on the NBS scale,  
1027 *Marine Chemistry*, 21, 315–327, 1987b.  
1028  
1029 Pérez, F. F., Rios, A. F., and Rosón, G.: Sea surface carbon dioxide off the Iberian  
1030 Peninsula North Eastern Atlantic Ocean, *Journal of Marine Systems*, 19, 27–46, 1999.  
1031  
1032 Perez, F. F., Alvarez-Salgado, X. A., and Rosón G.: Stoichiometry of the net ecosystem  
1033 metabolism in a coastal inlet affected by upwelling. The Ría de H (NW Spain), *Marine*  
1034 *Chemistry*, 69, 3-4, 217–236, 2000.  
1035  
1036 Pérez, F. F., Padin, X. A., Pazos, Y., Gilcoto, M., Cabanas, M., Pardo, P. C., Doval, M.,  
1037 D., and Farina-Busto, L.: Plankton response to weakening of the Iberian coastal  
1038 upwelling. *Global Change Biology*, 16(4), 1258–1267, 2010.



- 1039
- 1040 Pérez, F. F., Velo, A., Padin, X. A., Doval, M. D., Prego, R.: ARIOS DATABASE: An  
1041 Acidification Ocean Database for the Galician Upwelling Ecosystem,  
1042 Instituto de Investigaciones Marinas, Consejo Superior de Investigaciones Científicas  
1043 (CSIC), doi: 10.20350/digitalCSIC/12498, 2020.
- 1044
- 1045 Piedracoba, S., Alvarez-Salgado, X. A., Rosón G., and Herrera, J. L.: Short timescale  
1046 thermohaline variability and residual circulation in the central segment of the coastal  
1047 upwelling system of the Ría de Vigo (northwest Spain) during four contrasting periods,  
1048 <https://doi.org/10.1029/2004JC002556>, 2005.
- 1049
- 1050 Prego, R., Fraga, F., and Rios, A. F.: Water interchange between the Ria of Vigo and  
1051 the continental shelf. *Scientia Marina* 54, 95–100, 1990.
- 1052
- 1053 Raven, J., Caldeira, K., Elderfield, H., Hoegh-Guldberg, O., Liss, P., Riebesell, U.,  
1054 Sphepherd, J., Turley, C., and Watson, A.: Ocean acidification due to increasing  
1055 atmospheric carbon dioxide: Royal Society Policy Document 12/05, 68 p, 2005.
- 1056
- 1057 Ríos, A. F., Pérez, F. F., and Fraga, F.: Water masses in the upper and middle North  
1058 Atlantic Ocean east of the Azores, *Deep-Sea Res. Part I*, 39, 645–658, 1992.
- 1059
- 1060 Rosón, G., Pérez, F. F., Alvarez-Salgado, X. A., and Figueiras, F. G.: Variation of both  
1061 thermohaline and chemical properties in an estuarine upwelling ecosystem -Ría de  
1062 Arousa. 1. Time evolution, *Estuarine Coastal and Shelf Science*, 41, 2, 195–213, doi  
1063 10.1006/ecss.1995.0061, 1995.
- 1064
- 1065 Rosón, G., Cabanas, J. M., Pérez, F. F., Herrera, J. L., Ruiz-Villarreal, M., Castro, C.  
1066 G., Piedracoba, S., and Álvarez-Salgado, X. A.: Evidencias do cambio climático na  
1067 Hidrografía e a dinámica das Rías e da plataforma galega. Edita: Xunta de Galicia.  
1068 Consellería de Medio Ambiente e Desenvolvemento Sostible, Evidencias e impactos do  
1069 cambio climático en Galicia, 287-302, 2009.
- 1070
- 1071 Sabine, C. L., Feely, R. A., Gruber, N., Key, R. M., Lee, K., Bullister, J. L.,  
1072 Wanninkhof, R., Wong, C. S., Wallace, D. W. R., Tilbrook, B., Millero, F. J., Peng, T.-





- 1073 H., Kozyr, A., Ono, T., and Rios, A. F.: The oceanic sink for anthropogenic CO<sub>2</sub>.  
1074 Science 305, 367–371, 2004.  
1075
- 1076 Sarmiento, J. L., and Gruber, N.: Ocean biogeochemical dynamics. Princeton Univ.  
1077 Press. 2006.  
1078
- 1079 Souto, C., Gilcoto, M., Fariña-Busto, L., and Pérez, F. F.: Modeling the residual  
1080 circulation of a coastal embayment affected by wind-driven upwelling: Circulation of  
1081 the Ria de Vigo (NW Spain), Journal of Geophysical Research - Oceans, 108 C11  
1082 (3340), doi: 10.1029/2002JC001512, 2003.  
1083
- 1084 SCOR-UNESCO: Determination of Photosynthetic Pigments in Seawater. UNESCO,  
1085 Paris, 1966.  
1086
- 1087 Strickland, J. D. H., and Parsons, T.R.: A practical handbook of seawater analysis,  
1088 Fisheries Research Board of Canada, Ottawa, Ontario, 1972.  
1089
- 1090 Takeshita, Y., Frieder, C. A., Martz, T. R., Ballard, J. R., Feely, R. A., Kram, S., Nam,  
1091 S., Navarro, M. O., Price, N. N., and Smith, J. E.: Including high-frequency variability  
1092 in coastal ocean acidification projections, Biogeosciences, 12(19), 5853–5870,  
1093 doi:10.5194/bg-12-5853-2015, 2015.  
1094
- 1095 Teira, E., Martínez-García, S., Lonborg, C., and Álvarez-Salgado, X. A.: Growth rates  
1096 of different phylogenetic bacterioplankton groups in a coastal upwelling system,  
1097 Environmental microbiology reports, 1,6, 545–554, <https://doi.org/10.1111/j.1758-2229.2009.00079.x>, 2009.  
1098  
1099
- 1100 UNESCO: Background papers and supporting data on the Practical Salinity Scale 1978.  
1101 UNESCO Tech. Papers in Marine Science, 37, 144pp, 1981.  
1102
- 1103 Upström, L. R.: Boron = Chlorinity ratio of deep-sea water from Pacific Ocean, Deep-  
1104 Sea Res., 21, 161–162, 1974.  
1105



- 1106 Van Heuven, S., Pierrot, D., Rae, J.W.B., Lewis, E., Wallace, D.W.R. MATLAB  
1107 Program Developed for CO<sub>2</sub> System Calculations. ORNL/CDIAC-105b. Carbon  
1108 Dioxide Information Analysis Center, Oak Ridge National Laboratory, U.S. Department  
1109 of Energy, Oak Ridge, Tennessee, 2011.  
1110
- 1111 Velo, A., Pérez, F.F., Lin, X., Key, R.M., Tanhua, T., de la Paz, M., Olsen, A., van  
1112 Heuven, S., Jutterström, S., Ríos, A.F.: CARINA data synthesis project: pH data scale  
1113 unification and cruise adjustments, *Earth Syst. Sci. Data*, 2, 133–155, doi:10.5194/essd-  
1114 2-133-2010, 2010.  
1115
- 1116 Velo, A., Cacabelos, J., Pérez, F.F., Ríos, A.F.: GO-SHIP Software and Manuals:  
1117 Software packages and best practice manuals and knowledge transfer for sustained  
1118 quality control of hydrographic sections in the Atlantic. (Version v1.0.0), Zenodo,  
1119 <http://doi.org/10.5281/zenodo.2603122>, 2019.  
1120
- 1121 Villaceros-Robineau, N., Zúñiga, D., Barreiro-González, B., Alonso-Pérez, F.,  
1122 de la Granda, F., and Froján, M.: Bottom boundary layer and particle dynamics in an  
1123 upwelling affected continental margin (NW Iberia), *Journal of Geophysical Research:*  
1124 *Oceans*, 124, <https://doi.org/10.1029/2019JC015619>, 2019.  
1125
- 1126 Wahl, M., Saderne, V., and Sawall, Y.: How good are we at assessing the impact of  
1127 ocean acidification in coastal systems? Limitations, omissions and strengths of  
1128 commonly used experimental approaches with special emphasis on the neglected role of  
1129 fluctuations, *Mar. Freshw. Res.*, 67, 25–36, doi:10.1071/MF14154, 2016.  
1130
- 1131 Wolf-Gladrow, D. A., Riebesell, U., Burkhardt, S., and Bijma, J.: Direct effects of CO<sub>2</sub>  
1132 concentration on growth and isotopic composition of marine plankton, *Tellus*, 51B, 461,  
1133 1999.  
1134
- 1135 Wooster, W. S., Bakun, A., and McClain, D. R.: The seasonal upwelling cycle along the  
1136 eastern boundary of the North Atlantic, *Journal of Marine Research*, 34, 131–141, 1976.  
1137
- 1138 Zúñiga, D., Villaceros-Robineau, N., Salgueiro, E., Alonso-Pérez, F., Rosón, G.,  
1139 Abrantes, F., and Castro, C. G.: Particle fluxes in the NW Iberian coastal upwelling



1140 system: Hydrodynamical and biological control. *Continental Shelf Research*, 123  
1141 (2016), 89–98, <http://dx.doi.org/10.1016/j.csr.2016.04.008>, 2016.

1142

1143 Zúñiga, D., Santos, C., Froján, M., Salgueiro, E., Rufino, M. M., de la Granda, F.,  
1144 Figueiras, F. G., Castro, C. G., and Abrantes, F.: Diatoms as a paleoproductivity proxy  
1145 in the NW Iberian coastal upwelling system (NE Atlantic), *Biogeosciences*, 14, 1165–  
1146 1179, [www.biogeosciences.net/14/1165/2017](http://www.biogeosciences.net/14/1165/2017), 2017.

1147

1148

1149

1150

1151

1152

1153

1154

1155

1156

1157

1158

1159

1160

1161

1162

1163

1164

1165

1166

1167

1168

1169

1170

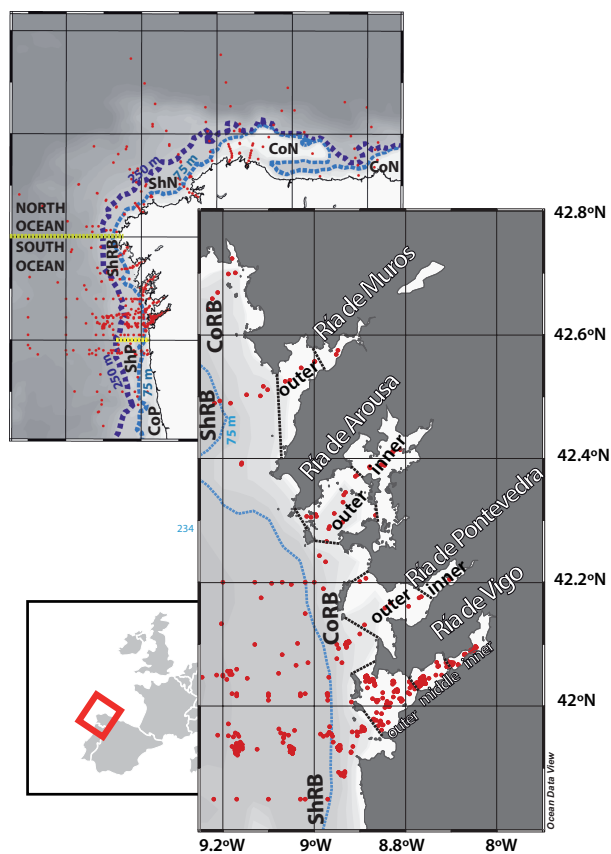
1171

1172

1173



1174



1175

1176

1177 Figure 1. Map of all stations (red dots) including the geographical areas selected to  
1178 classify the ARIOS database from isobath of 250 m (dark blue line) and 75 metres (light  
1179 blue line), latitudinal criterion (yellow lines) and geographical lines (black lines).

1180

1181

1182

1183

1184

1185

1186

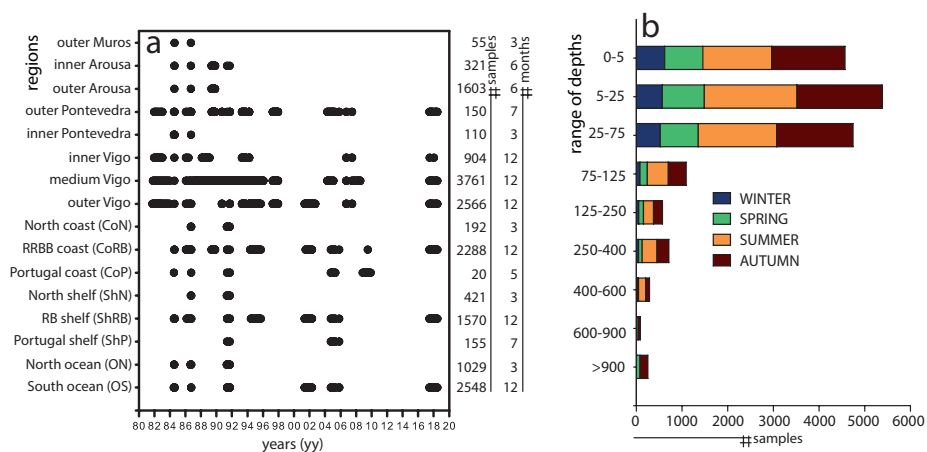
1187

1188



1189

1190



1191

1192

1193 Figure 2. a) Temporal distribution of the observations in the geographical boxes

1194 included in the ARIOS dataset. b) Seasonal distribution of the measurements in relation

1195 to depth.

1196

1197

1198

1199

1200

1201

1202

1203

1204

1205

1206

1207

1208

1209

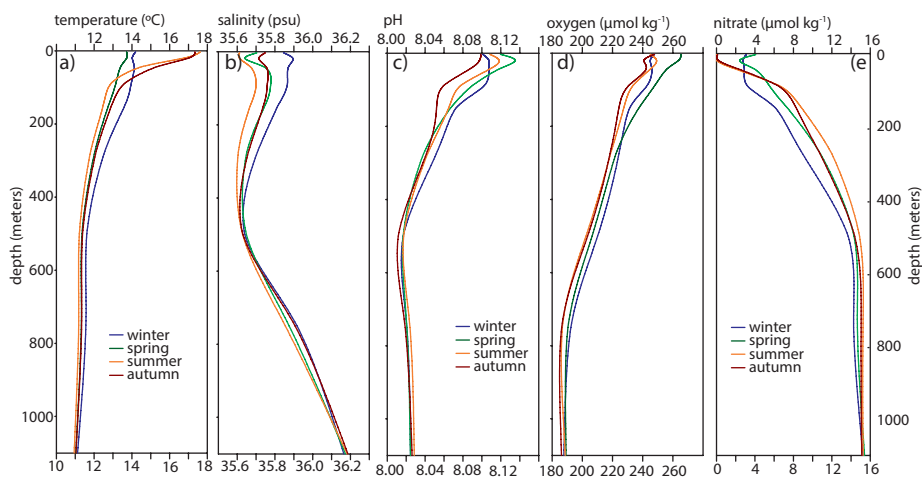
1210

1211

1212



1213  
1214  
1215



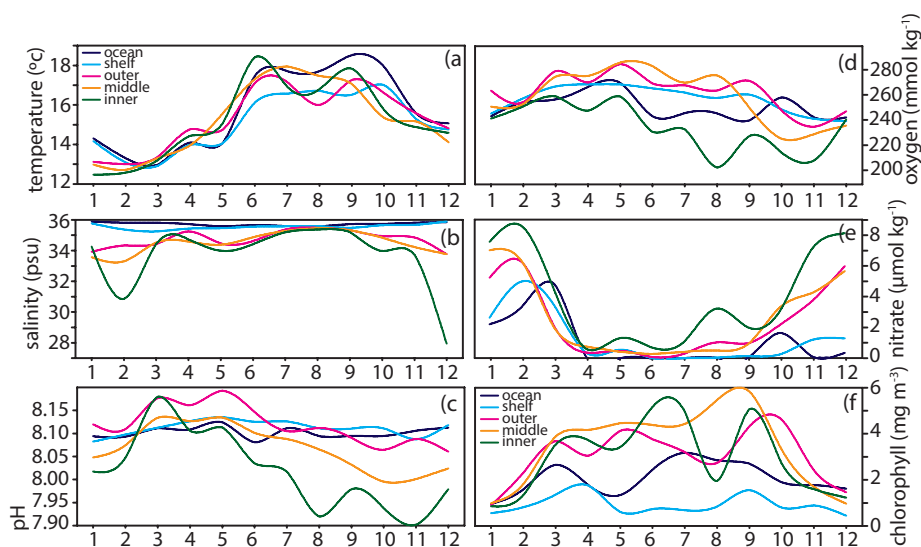
1216  
1217

1218 Figure 3. Profiles of seasonal means of temperature (a), salinity (b), pH (c), oxygen (d)  
1219 and nitrate concentration (e) in the first 1100 meters of the region South Ocean shown  
1220 in Fig. 1.

1221  
1222  
1223  
1224  
1225  
1226  
1227  
1228  
1229  
1230  
1231  
1232  
1233  
1234  
1235  
1236



1237  
1238  
1239  
1240



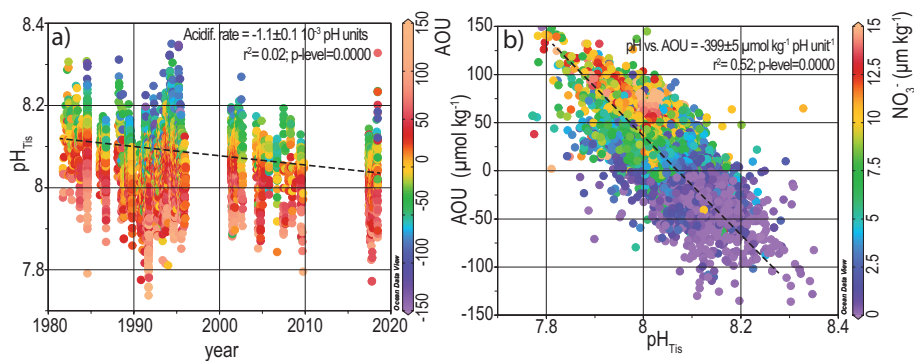
1241  
1242  
1243  
1244  
1245  
1246  
1247

Figure 4. Sea surface (<5 meters depth) seasonal cycles in 1976 - 2018 of temperature (a), salinity (b), pH (c), oxygen concentration (d), nitrate concentration (e) and chlorophyll (f) at sea surface for five geographical boxes shown in Fig. 1: South Ocean, RB shelf and outer, middle and inner Ria de Vigo for the entire period of the ARIOS database.

1248  
1249  
1250  
1251  
1252  
1253  
1254  
1255  
1256  
1257  
1258



1259  
1260  
1261  
1262



1263  
1264  
1265  
1266  
1267  
1268  
1269  
1270  
1271  
1272  
1273  
1274  
1275  
1276  
1277  
1278  
1279  
1280  
1281  
1282  
1283  
1284

Figure 5. Time-series of pH ARIOS data. The black line depicts the long-term trend. Scatter diagram of AOU vs pH including the nitrate concentration shown as colour of every dot.





EXPCODE	PROJECT	DATE	IP	#	CTD	O <sub>2</sub>	Nut	pH	Alk	Chla	CRM	Data Repository	REGIONS
29LP19761026	Ria Vigo 1977	1976-10-26	F Fraga	135	N	N	S*	S°	N	N	N	http://dx.doi.org/10.20350/digitalCSIC/9917	C <sub>0</sub> <sup>RB</sup>
29LP19810929	Ria Vigo 1981-83	1981-09-29	F Fraga	748	N	S*	S*	S°	S	N	N	http://dx.doi.org/10.20350/digitalCSIC/9918	RV <sup>O,MI</sup>
29LP19830215	Ria Vigo 1983-84	1983-02-15	F Fraga	312	N	S*	S*	S°	S	N	N	http://dx.doi.org/10.20350/digitalCSIC/9919	RV <sup>O,M</sup>
29GD19840711	GALICIA-VIII	1984-07-11	F Fraga	1865	N	S	S	S°	S	S	N	http://dx.doi.org/10.20350/digitalCSIC/9908	O <sup>NS</sup> , SH <sup>RB</sup> , C <sub>0</sub> <sup>P,RB</sup> , RV <sup>O,MI</sup> , RA <sup>O,I</sup> , RP <sup>O,I</sup> , RM
29GD19860121	Ria Vigo 1986	1986-01-21	F Fraga	332	N	S	S	S°	S	S	N	http://dx.doi.org/10.20350/digitalCSIC/9910	SH <sup>RB</sup> , C <sub>0</sub> <sup>RB</sup> , RV <sup>O,MI</sup>
29GD19860904	GALICIA-IX	1986-09-04	F Fraga	1640	N	S	S	S°	S	S	N	http://dx.doi.org/10.20350/digitalCSIC/9911	O <sup>NS</sup> , SH <sup>P,RB,N</sup> , C <sub>0</sub> <sup>P,RB,N</sup> , RV <sup>O,MI</sup> , RA <sup>O,I</sup> , RP <sup>O,I</sup> , RM
29LP19870120	PROVIGO	1987-01-20	FF Pérez	2317	N	S	S	S°	N	S	N	http://dx.doi.org/10.20350/digitalCSIC/9924	RV <sup>M</sup>
29LP19880212	LUNA 88	1988-02-12	AF Rios	468	N	S	S	S°	S	S	N	http://dx.doi.org/10.20350/digitalCSIC/9907	RV <sup>M,I</sup>
29IN19890512	GALICIA-X	1989-05-12	FF Pérez	3113	N	S	S	S°	S	S	N	http://dx.doi.org/10.20350/digitalCSIC/9920	C <sub>0</sub> <sup>RB</sup> , RA <sup>O,I</sup>
29IN19900914	Ria Vigo 1990	1990-09-14	FG Figueiras	108	Y	S	S	S°	S	S	N	http://dx.doi.org/10.20350/digitalCSIC/9921	RV <sup>O,MI</sup>
29IN19910510	GALICIA-XI	1991-05-10	FF Pérez	327	Y	S	S	S°	S	S	N	http://dx.doi.org/10.20350/digitalCSIC/9922	O <sup>NS</sup> , SH <sup>P,RB,N</sup> , C <sub>0</sub> <sup>P,RB,N</sup> , RA <sup>O</sup>
29IN19910910	GALICIA-XII	1991-09-10	FG Figueiras	663	Y	S	S	S°	S	S	N	http://dx.doi.org/10.20350/digitalCSIC/9923	O <sup>NS</sup> , SH <sup>P,RB,N</sup> , C <sub>0</sub> <sup>P,RB,N</sup> , RV <sup>O,MI</sup> , RA <sup>O</sup>
29LP19930413	Ria Vigo 1993-94	1993-04-13	FG Figueiras	406	Y	S	S	S°	S	S	N	http://dx.doi.org/10.20350/digitalCSIC/9927	RV <sup>O,MI</sup>
29JN19940505	Ria Vigo 1994-95	1994-05-05	MCabanas	669	Y	S	S	S°	S	S	N	http://dx.doi.org/10.20350/digitalCSIC/9926	SH <sup>RB</sup> , C <sub>0</sub> <sup>RB</sup> , RV <sup>O</sup>
29MY19970407	CIRCA-97	1997-04-07	FF Pérez	547	Y	S	N	S°	S	S	N	http://dx.doi.org/10.20350/digitalCSIC/9928	RV <sup>O,MI</sup>
29MY20010515	DYBAGA	2001-05-15	FF Pérez	1421	Y	S	S*	S	S	S	Y	http://dx.doi.org/10.20350/digitalCSIC/9929	SH <sup>P,RB</sup> , C <sub>0</sub> <sup>RB</sup> , RV <sup>O</sup>
29MY20010702	REMODA	2001-07-02	XA Alvarez	203	Y	S	S*	S	S	S	Y	http://dx.doi.org/10.20350/digitalCSIC/9930	RV <sup>O</sup>
29MY20040419	FLUVBE	2004-04-19	CG Casiro	187	Y	S	S*	S	S	S	Y	to be submitted	RV <sup>M,I</sup>
29CS20041004	ZOTRACOS	2004-10-04	MCabanas	371	Y	S	S	S	S	S	Y	http://dx.doi.org/10.20350/digitalCSIC/9932	SH <sup>P,RB</sup> , C <sub>0</sub> <sup>RB</sup> , RP <sup>O</sup>
29MY20060926	CRIA	2006-09-26	D Barton	197	Y	S	S*	S	S	S	Y	http://dx.doi.org/10.20350/digitalCSIC/9931	RV <sup>O,MI</sup>
29MY20070917	RAFTING	2007-09-17	CG Casiro	287	Y	S	S*	S	S	S	Y	to be submitted	RV <sup>M</sup>
29MY20081105	LOCO	2008-11-05	XA Alvarez	72	Y	S	S	S	S	S	Y	http://dx.doi.org/10.20350/digitalCSIC/9936	C <sub>0</sub> <sup>RB</sup>
29AH20090710	CAIBEX-I	2009-07-10	D Barton	191	Y	S	S	S	S	S	Y	http://dx.doi.org/10.20350/digitalCSIC/9934	C <sub>0</sub> <sup>P,RB</sup>
29MY20170609	ARIOS	2017-06-09	FF Pérez	1114	Y	S	S*	S	S	S	Y	http://dx.doi.org/10.20350/digitalCSIC/9963	SH <sup>P,RB</sup> , C <sub>0</sub> <sup>RB</sup> , RV <sup>O,MI</sup>



1285 Table 1. Discrete measurements of projects gathered in the ARIOS database and  
1286 associated information: including dates, sample number (#), the principal investigator  
1287 (PI), measured parameters, link to data repository and the sampled geographical area.  
1288  
1289 - All projects include measurements of *T*, *S*. Others as *pH*, alkalinity (*Alk*), nutrient  
1290 (*Nut*), oxygen (*O<sub>2</sub>*) concentration, chlorophyll (*Chla*) are indicated.  
1291 - The concentration units of these variables are  $\mu\text{mol kg}^{-1}$  or  $\mu\text{mol L}^{-1}$  (\*) and the *pH*  
1292 measurements in NBS scale (°) or in total scale.  
1293 - Regions are identified as ocean (*O*), shelf (*Sh*), coastal (*Co*), Ría de Vigo (*RV*), Ría de  
1294 Pontevedra (*RP*), Ría de Arousa (*RA*) and Ría de Muros (*RM*) while the superscript  
1295 index means south (<sup>*S*</sup>), north (<sup>*N*</sup>), Portugal (<sup>*P*</sup>), Rías Baixas (<sup>*RB*</sup>), outer (<sup>*O*</sup>), middle (<sup>*M*</sup>)  
1296 and inner (<sup>*I*</sup>).  
1297  
1298  
1299  
1300  
1301  
1302  
1303  
1304  
1305  
1306  
1307  
1308  
1309  
1310  
1311  
1312  
1313  
1314  
1315  
1316  
1317  
1318



1319

	$SS_{range}$	$r^2_{ss}$	$t_{interannual}$	$r^2$	p-value
OCEAN	0.050	0.17	-0.0012±0.0002	0.21	0.0000
SHELF	0.050	0.06	-0.0017±0.0003	0.15	0.0009
OUTER	0.120	0.24	-0.0027±0.0003	0.21	0.0000
MIDDLE	0.130	0.28	-0.0022±0.0005	0.03	0.0000
INNER	0.260	0.47	-0.0039±0.0005	0.34	0.0000

1320

1321 Table 2: Seasonal amplitude of monthly pH means ( $SS_{range}$ ) and long-term trends  
1322 ( $t_{interannual}$ ) of pH in five regions and significant regression coefficients between the in  
1323 situ pH measurements and the monthly mean pH values ( $r^2_{ss}$ ) and the regression  
1324 coefficient of the temporal variability of the deseasonalized pH measurements ( $r^2$ ).

1325

1326

1327

1328

1329